FACULTADE DE QUÍMICA

GRAO EN QUÍMICA

VISIBLE-LIGHT PROMOTED BIOORTHOGONAL PHOTOCATALYSIS

LARA TRONCOSO AFONSO

2020-2021

UNIVERSIDADE DE SANTIAGO DE COMPOSTELA

TRABALLO FIN DE GRAO

Rama de coñecemento: Química Orgánica.

Departamento, centro, institución ou empresa: Centro de Investigación en Química Biolóxica e Materiais Moleculares (CiQUS).

Titor: José Luis Mascareñas Cid

Cotitora: María Tomás Gamasa

Autorización dos titores:

D. José Luis Mascareñas Cid, Catedrático do Departamento de Química Orgánica da Universidade de Santiago de Compostela.

Dra. María Tomás Gamasa, Investigadora JIN do Departamento de Química Orgánica da Universidade de Santiago de Compostela.

Certifican: que a presente memoria adxunta, titulada ‘’*Visible-light promoted bioorthogonal photocatalysis*’’, que presenta Lara Troncoso Afonso, foi realizada baixo a súa dirección nos laboratorios do Centro Singular de Investigación en Química Biolóxica e Materiais Moleculares (CiQUS).

Considerando que a nomeada memoria constitúe o seu traballo fin de grado, autorizan a súa presentación na Universidade de Santiago de Compostela.

Para que así conste, firman o presente informe en Santiago de Compostela a día 5 de Xullo de 2021.

MASCAREÑAS CID JOSE LUIS - 34934771W
Firmado digitalmente por MASCAREÑAS CID JOSE LUIS - 34934771W
Fecha: 2021.07.05 10:21:47 +02'00'

TOMAS GAMASA MARIA - 09417809E
Firmado digitalmente por TOMAS GAMASA MARIA - 09417809E
Fecha: 2021.07.05 10:33:56 +02'00'

AGRADECEMENTOS

Desculpándome de antemán por si esquezo mencionar alguén, gustaríame agradecer a todas as persoas que me apoiaron ao longo da miña formación:

En primeiro lugar, a Xulián, María e José Luis pola implicación, apoio e dedicación ao longo do desenvolvemento do presente traballo. Seguidamente, a todos os profesores que durante estes anos foron quen de transmitirme a súa curiosidade científica e afán pola química.

Finalmente, á miña familia en xeral e, en particular, a meus pais polo apoio incondicional, á miña irmá Carlota por sacar o mellor de min e ás miñas avoas, Carmen e Pilar, por ser os meus máis valiosos exemplos de esforzo, perseverancia e traballo constante dende nena.

TABLE OF CONTENTS

ABSTRACT

Biological chemistry deals with the study of the chemical processes that occur inside living beings, from a molecular perspective. Understanding the cellular and molecular mechanisms underlying biological functions is fundamental for the treatment of many diseases. Furthermore, being able to manipulate, monitor and transform cellular behaviour is key to the development of modern medicine.

However, interfering with cell's functioning is not a trivial task and it requires the development of tools to carry out designed transformations under the complex environment of biological habitats. The chemical transformation of exogenous or endogenous substances inside living beings requires bioorthogonality and selectivity. One way to perform biocompatible reactions could be based on the use of photochemically-induced transformations, promoted by visible light.

Combining photochemistry and bioorthogonal methods leads to bioorthogonal photochemistry, a new field of research that is still in its infancy. During this TFG, some preliminary work in this area have been carried out.

RESUMEN

La química biológica consiste en el estudio de los procesos químicos que ocurren en el interior de los seres vivos desde el punto de vista molecular. Entender los mecanismos celulares y moleculares relativos a las funciones biológicas es fundamental para el tratamiento de muchas enfermedades. Es más, ser capaz de manipular, monitorizar y transformar el comportamiento celular es clave para el desarrollo de la medicina moderna.

Sin embargo, interferir en las funciones celulares no es una tarea trivial y requiere el desarrollo de nuevas herramientas para llevar a cabo las transformaciones diseñadas bajo el complejo ambiente de los sistemas biológicos. Las transformaciones químicas de sustancias exógenas o endógenas en el interior de los seres vivos requiere

bioortogonalidad y selectividad. Un modo de llevarlas a cabo podría basarse en el uso de transformaciones inducidas fotoquímicamente, promovidas por la luz visible.

La combinación de la fotoquímica y los métodos bioortogonales abre paso a la química fotobioortogonal, un novedoso campo de investigación que se encuentra todavía en su infancia. Durante este TFG, se ha llevado a cabo trabajo preliminar en este área.

RESUMO

A química biolóxica consiste no estudo dos procesos químicos que acontecen no interior dos seres vivos para entender os seres vivos dende o punto de vista molecular. Entender os mecanismos celulares e moleculares relativos as funcións biolóxicas é fundamental para o tratamento de moitas enfermidades. É máis, ser capaz de manipular, monitorizar e transformar o comportamento celular é clave para o desenvolvemento da medicina moderna.

Non obstante, interferir nas funcións celulares non é unha tarefa trivial e require o desenvolvemento de novas ferramentas para levar a cabo as transformacións deseñadas baixo o complexo ambiente dos sistemas biolóxicos. As transformacións químicas de substancias exóxenas e endóxenas no interior dos seres vivos require bioortogonalidade e selectividade. Un modo de levalas a cabo podería basearse no uso de transformacións inducidas fotoquímicamente, promovidas pola luz visible.

A combinación da fotoquímica e os métodos bioortogonales abre paso a química fotobioortogonal, un novidoso campo de investigación que se encontra aínda na súa infancia. Durante este TFG, levouse a cabo traballo preliminar nesta área.

1. INTRODUCTION

1.1. Bioorthogonal chemistry

Bioorthogonal chemistry refers to a series of quick, nonnative abiotic chemical reactions that occur in complex biological environments. Moreover, for these transformations to be considered bioorthogonal, they need to be carried out with good selectivity in the presence of biological components. [1; 2]

The development of this type of biocompatible chemical reactions is not trivial. While the first examples of bioorthogonal reactions reported were restricted to the modification of nucleophilic amino acids (e.g., cysteines), today many other options are available, including catalytic methods based on transition metal reagents. [3]

In nature, many transformations in complex physiological conditions and inside cells are mediated by enzymes and metalloenzymes. These natural catalysts are implied in all the vital functions of living organisms. Chemists have been trying for years to obtain artificial versions of enzymes to catalyze nonnative reactions in a bioorthogonal manner. Research on this area has led to the design of different artificial metalloenzymes with relatively good success. [4; 5]

One alternative to carry out bioorthogonal reactions in live settings is based on the use of discrete transition metal catalysts. These artificial catalysts can promote a great variety of reactions in biological systems and also in cells, as for example, gold-promoted hydroarylations or ruthenium isomerizations, as demonstrated by our group. [6; 7]

There are other metal-free bioorthogonal reactions such as Staudinger ligations, inverse electron-demand Diels Alder reactions or cycloadditions promoted by light. In general, the complexity of physiological media, with different concentration of salts, biomolecules and ions, makes the development of bioorthogonal methods really challenging. There are mainly two types of transformations: bioorthogonal ligation reactions (*figure 1*) and bioorthogonal cleavage reactions (*figure 4*).

1.1.1. Bioorthogonal ligation reactions

This type of strategies were the first so far developed. Staudinger azide-triphenylphosphine ligation, inverse electron-demand Diels-Alder reactions and copper catalyzed azide-alkyne cycloadditions were the pioneering bioorthogonal ligations and their applications were focused on the labelling biomolecules, and on the synthesis of sophisticated pharmaceuticals. [8] Nevertheless, these reactions were only the starting point of a large number of bioorthogonal processes that have been developed over the last years.

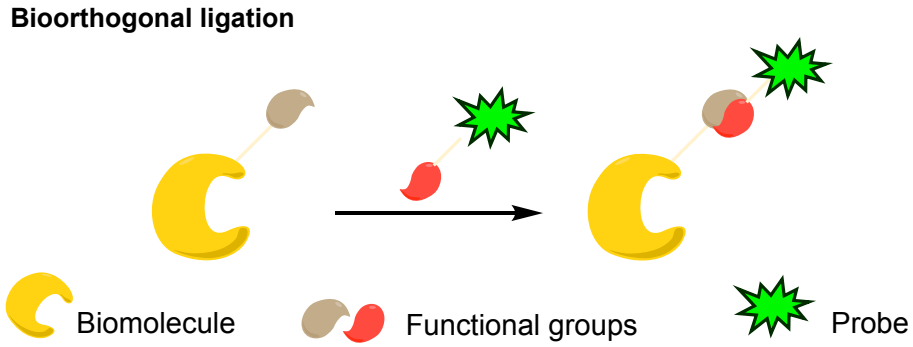

Figure 1 Scheme for bioorthogonal ligation processes. [8]

In general, metal complexes are really versatile agents for promoting chemical transformations as they allow to change not only the main metal but also the ligands coordinated to the central cation. In other words, they can be designed with specific physical and chemical characteristics and therefore, they can be adapted to different reaction media by changing its solubility or to different substrates by modulating the electron-donor character of the complex. This flexibility led chemists to consider the utility of this complexes to perform bioorthogonal ligations. Cross-coupling of biomolecules catalyzed by palladium (e.g. Suzuki-Miyaura [9], Sonogashira reactions [10]…) or cross-metathesis reactions catalyzed by ruthenium [11] constitute some examples. Albeit the more famous is the copper-catalyzed cycloaddition between alkynes and azides.

Over the years, strategies to avoid the use of copper in bioorthogonal reactions have been developed. This is due to its toxicity and instability in the presence of O_2 and H_2O_2.

These problems led to the development of azide-alkyne cycloadditions promoted by strain (SPAAC, *figure 2*). This reaction requires the use of an internal alkyne (the smallest one available is cyclooctyne) and a dipole, such as azide, nitrile oxide or nitrone groups. This strategy was first stablished by Bertozzi and coworkers, and the applications are mainly focused on labeling biomolecules, as for example the labeling of proteins and glycans for visualization of living melanoma cells. [12] Nevertheless, the reaction rate of this transformation is low and cyclooctynes are instable and rather commercially available, so chemists kept on looking for alternatives.

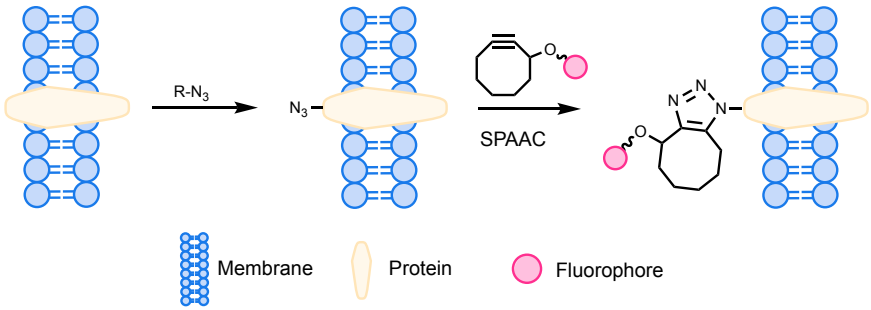

Figure 2 Scheme for SPAAC reaction. [8]

Other bioorthogonal strategies are photoclick reactions, in which light is used as a source of energy to induce the formation of reactive radicals that undergo the desired reaction. These processes can be highly controlled by changing the wavelength and intensity of radiation source. Prompt examples are the photoinduced 1,3-dipolar cycloaddition between tetrazoles and alkenes to label proteins in biological media [13] or even glucagon receptors inside living mammalian cells. [14] As it is showed in *figure 3* the driving force of the reaction is the release of N_2 to generate a dipole *in situ* that reacts with the alkene to give pyrazoline derivatives.

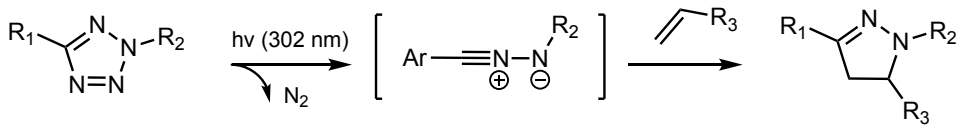

Figure 3 Reaction scheme for 1,3-dipolar cycloaddition between tetrazoles and alkenes. [8]

Another photoclick method is the [4+2] cycloaddition promoted by light between 9,10-phenanthrenequinone and electron-rich alkenes described by Zhang and coworkers in 2018, a suitable strategy for spatial and temporal labeling of living cells. [15]

1.1.2. Bioorthogonal cleavage reactions

In general, cleaving bonds usually implies strong acidic, basic, nucleophilic, oxidizing or reducing conditions and the use of these common strategies in biological media is limited. Nevertheless, chemists have successfully developed different methodologies based not only on milder acids, nucleophiles or redox processes but also involving transition metals or light. [8]

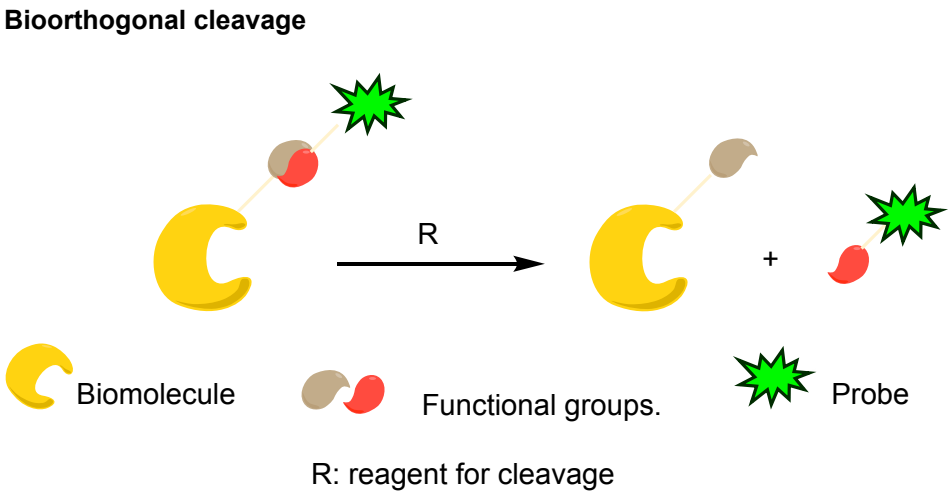

Figure 4 Scheme for bioorthogonal cleavage processes. [8]

Bioorthogonal cleavage reactions were principally developed by modifying the linking strategies explained above. Most common types of molecules that can be released are fluorescent probes, biomolecules or pharmaceuticals. On the one hand, Staudinger reactions can be used for releasing molecules as shown in *figure 5*. The bioorthogonal methods based on Staudinger reactions take advantage of the mild electrophilic character of the azide group, rarely found in biological media, stable and nontoxic.

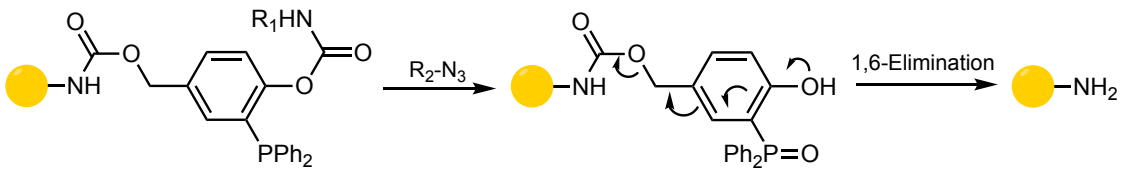

Figure 5 Example of molecular releasing via Staudinger reaction. [8]

On the other hand, metal-mediated deprotection processes, such as deallylation, and cycloaddition reactions can be used as well for bond cleaving as shown in *figure 6*.

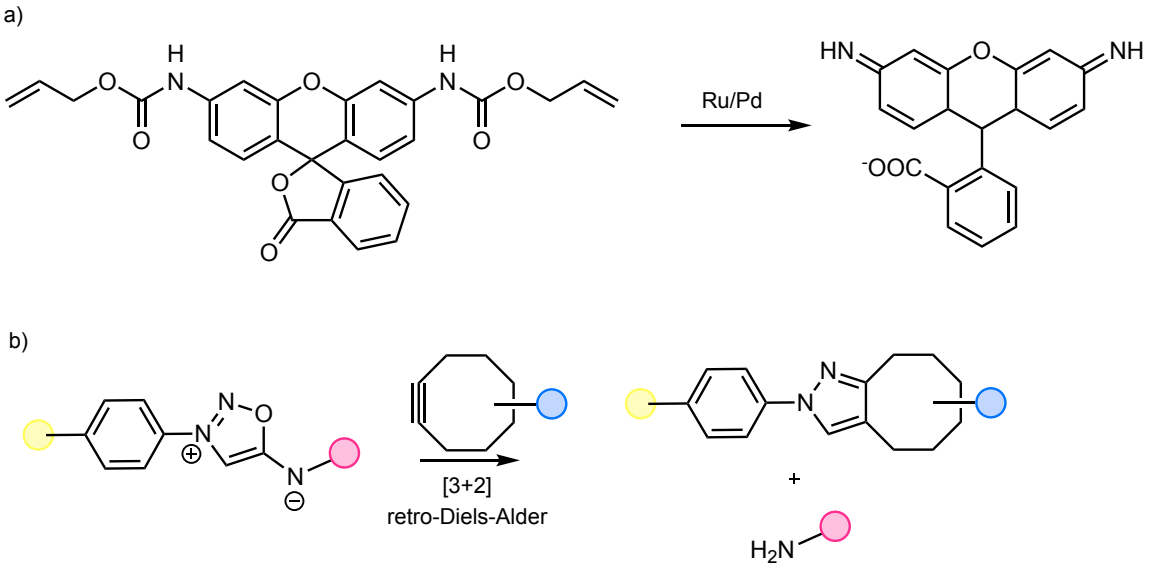

Figure 6 Molecular releasing induced by transition metals (a) or cycloaddition reactions (b). [8]

Finally, molecular releasing can be promoted by light. In this case, no other than photolabile groups are needed, and a relevant example is the sequential breakdown of a molecule controlled by using two different wavelengths and performed inside living cells by Chenoweth's group in 2018. [16]

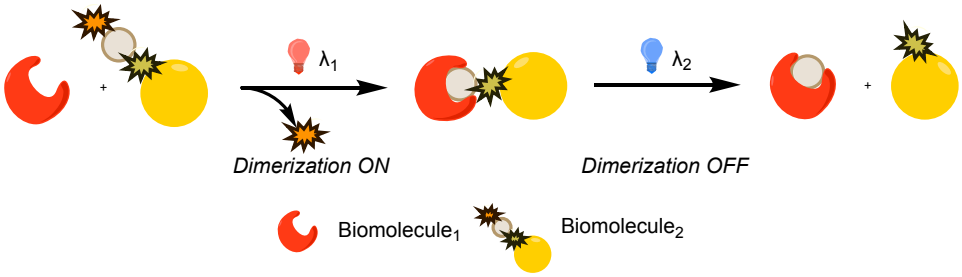

Figure 7 Schematic representation for wavelength dependent molecule's breakdown. [16]

1.1.3. Requirements for achieving bioorthogonality

As it might be deduced, achieving selectivity in a reaction media with loads of different functionalities is really challenging and bioorthogonal methods must satisfy particular requirements in comparison with common reactions carried out in laboratory flasks.

In concrete, for a reaction to be performed in biological environments, substrates must be abiotic, that is, they should be absent in common biological media. Moreover, the concentrations used must be low enough to avoid cytotoxicity issues but high enough to undergo the reaction in a cellular complex environment with restricted conditions of pH and temperature.

The development of this type of strategies usually involves four steps, after selecting a transformation which is susceptible of being translated to biological media. The first step involves the search of suitable reaction conditions as well as the evaluation of the selectivity and compatibility of the functional groups implied in the reaction, so this step is carried out in laboratory flasks. This is followed by a deeper study of complex reaction media, with large biomolecules and different functionalities present as well. The third step implies the investigation of the reaction in cells and finally, living organisms will be used to confirm the compatibility of the transformation with complex organisms (*figure 8*).

At this point, it is necessary to explore new and alternative sources of energy to promote unnatural transformations in biological media. In order to face this issue, visible light emerges as a powerful tool: it supplies energy while keeping cells integrity.

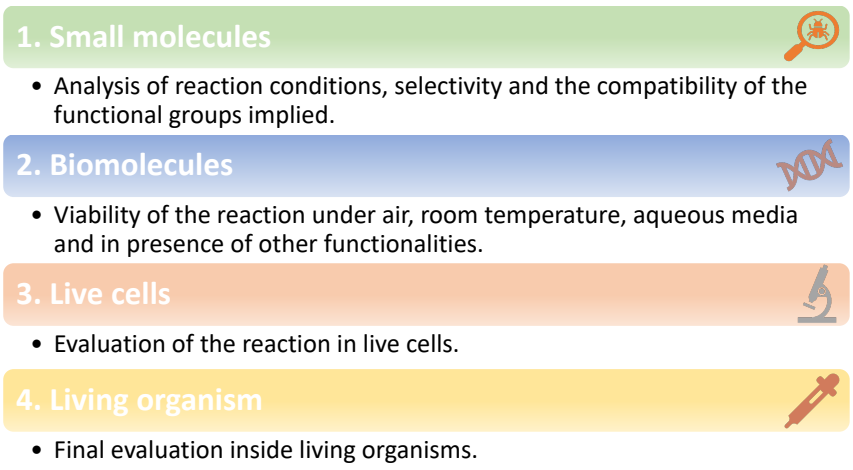

Figure 8 Main steps in the development of bioorthogonal strategies.[17]

1.2. Photocatalysis

Recently, interest in photocatalysis has experienced an important growth, specially that concerning visible light. Visible light radiation is a source of electrochemical energy and therefore, it allows the generation of new reactivity pathways mediated by electron transfer and radical processes.

Light can provide an alternative reaction pathway with a lower energy barrier. Furthermore, this energy stimuli presents other advantages. [18] First, high temperatures are no longer needed, and the only requirement is choosing the right excitation wavelength. Second, the selectivity of the reaction is enhanced as the desired substrate can be selectively excited in the presence of other chemical moieties. Third, using light as a source of energy allows the reaction to be temporally and spatially controlled. [19] Finally, light is a clean, renewable and abundant source of energy and, as a result, photoinduced reactions can be considered an ecological synthetic methodology. [18]

1.2.1. Photosensitization and photoredox catalysis

The main advantage of using visible light as source of energy is that usually photoactive substances (PA) absorb photons with lower wavenumber than other biomolecules ubiquitously present in physiological media. Consequently, it is possible to selectively transfer energy to a specific molecule and also to exert both temporal and spatial control of the reaction.

The first step for photochemical transformations is absorption of a photon causing molecules to occupy an excited state (S_1). Once in there, molecules return back to the fundamental state following two main paths: (a) intersystem crossing to T_1, a long-live forbidden state of energy, followed by deactivation through energy, electron or hydrogen atom transfer processes and (b) deactivation from S_1 through energy, electron or hydrogen atom transfer processes *(figure 9).* [20]

There are mainly two types of photochemical transformations: photosensitized and photoredox catalysis. The main difference is that photosensitization implies the energy transfer pathway while photoredox catalysis occurs through electron transfer.

On the one hand, photoredox catalysis implies electron transfer from the excited catalyst to substrate followed by regeneration of the catalyst due to reverse electron transfer process (closing the catalytic cycle). Nevertheless, in presence of enough oxygen, ROS (reactive oxygen species) can be generated after photon absorption causing the oxidation of other biomolecules present in cells. To avoid these interferences, it is important to sophistically control the reaction conditions (wavelength of the radiation, temperature, presence of oxygen…).

On the other hand, photosensitization processes can occur through two types of mechanisms: (a) excited photosensitizer gives a fraction of the energy absorbed to a neighbor biomolecule that reacts with oxygen giving the oxidized product; and (b) excited photosensitizer transmits energy directly to oxygen, resulting in reactive oxygen species (ROS) that oxidize the biomolecule. Moreover, mechanism (a) is favored as long as high concentrations of oxygen are present in the reaction media.

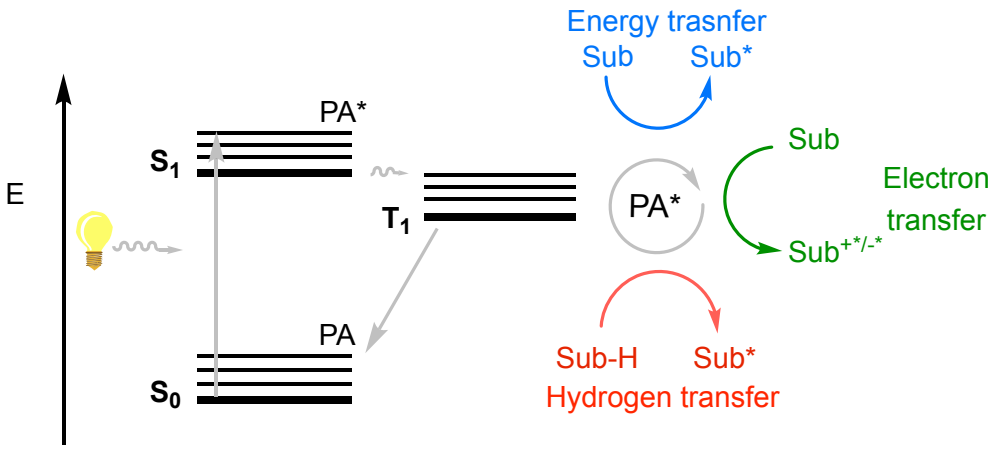

Figure 9 Scheme for illustrating different deactivation processes of molecules after excitation.

Photosensitization is used with clinical purposes in photodynamic therapy (PDT), a noninvasive and promising treatment for cancer based on the generation of ROS to cause cellular degradation. Scientific efforts to improve the efficiency and selectivity of

this treatment have led to three generations of photosensitizers, from simple natural occurring porphyrins to sophisticated aggregation-induced emission luminogens (AIEgens) and metal-organic frameworks (MOFs), going through the use of heavy-metal based sensitizers. [20]

1.2.2. Photocatalysis in water

Although the combination of photocatalysis and aqueous media can be considered a powerful tool to perform sustainable organic transformations, this is a field in its total infancy.

There are some photoinduced reactions that have been performed in water such as arylation of pyridines with aryldiazonium salts [21] (*figure 10a*), synthesis of trifluoromethylated dihydroisoquinolines [22] (*figure 10b*) or amide bond formation [23] (*figure 10c*). However, many transformations still require organic solvents, as some reactants are either poorly soluble in water or likely prone to suffer from hydrolysis. [18]

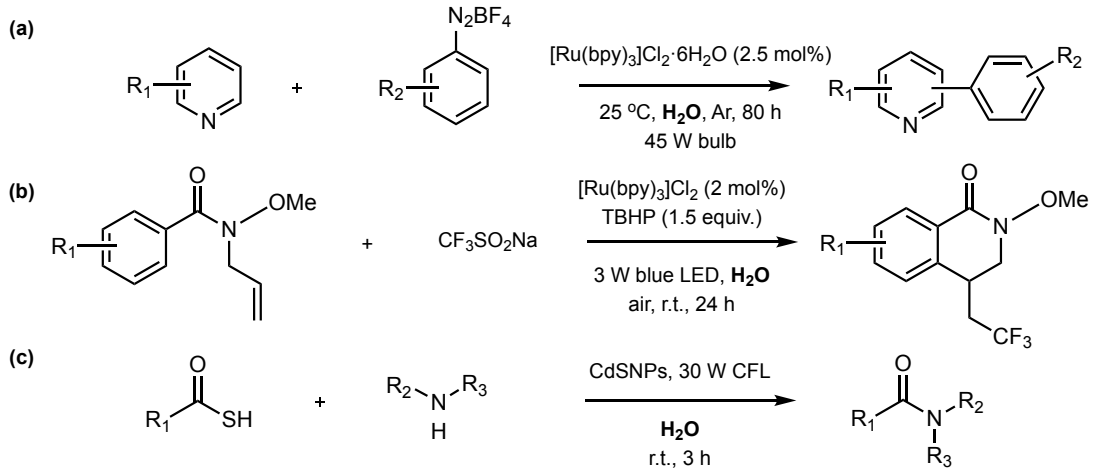

Figure 10 Examples of photoinduced transformations performed in water.

Substitution of traditional-based organic solvents by water reduces difficult-to-treat wastes and risks related to heat and gas release from the reaction. [18] Moreover, water is an abundant natural liquid, innocuous and it is ubiquitously present in all living organisms.

Therefore, using water as a solvent is not only ecological but also provides for developing biocompatible transformations. In fact, the development of photocatalytic synthetic strategies in water media is fundamental to discover light-induced bioorthogonal strategies.

1.2.3. Bioorthogonal photocatalysis

The maintenance of all the vital functions needed for an organism to stay alive requires a perfect functioning of the cellular enzymatic machinery. These natural biocatalysts are implied in cellular metabolism, respiration and reproduction enabling living beings to growth and stay healthy. In fact, alterations in enzymatic functions often trigger diseases and pathologic processes.

In this sense, absorption of light is a well-known natural method that living organisms use to activate their biocatalysts and this fact has inspired the development of artificial visible light induced catalysis inside cells. [20]

The combination of photocatalysis and bioorthogonal chemistry has led to the birth of a new field, bioorthogonal photochemistry, with great potential to face problems and foster progress in biomedical engineering, nanomaterials, nanomedicine, drug discovery and human health. [3; 20]

Curiously, although visible light is highly compatible with living systems, there are few applications of photochemical reactions in biology. Some of those reports include: fotoredox dimerization of tyrosines (*figure 11a*), [24] bioorthogonal photocatalyzed oxidation of a prodrug (*figure 11b*), [2] or photocatalyzed reduction of azides with bioimaging purposes (*figure 11c*). [25] The reason behind this scarcity might be related to the notion of incompatibility between radical chemistry and biological environments as well as to the need of using cell-damaging UV-light to promote photochemical reactions.

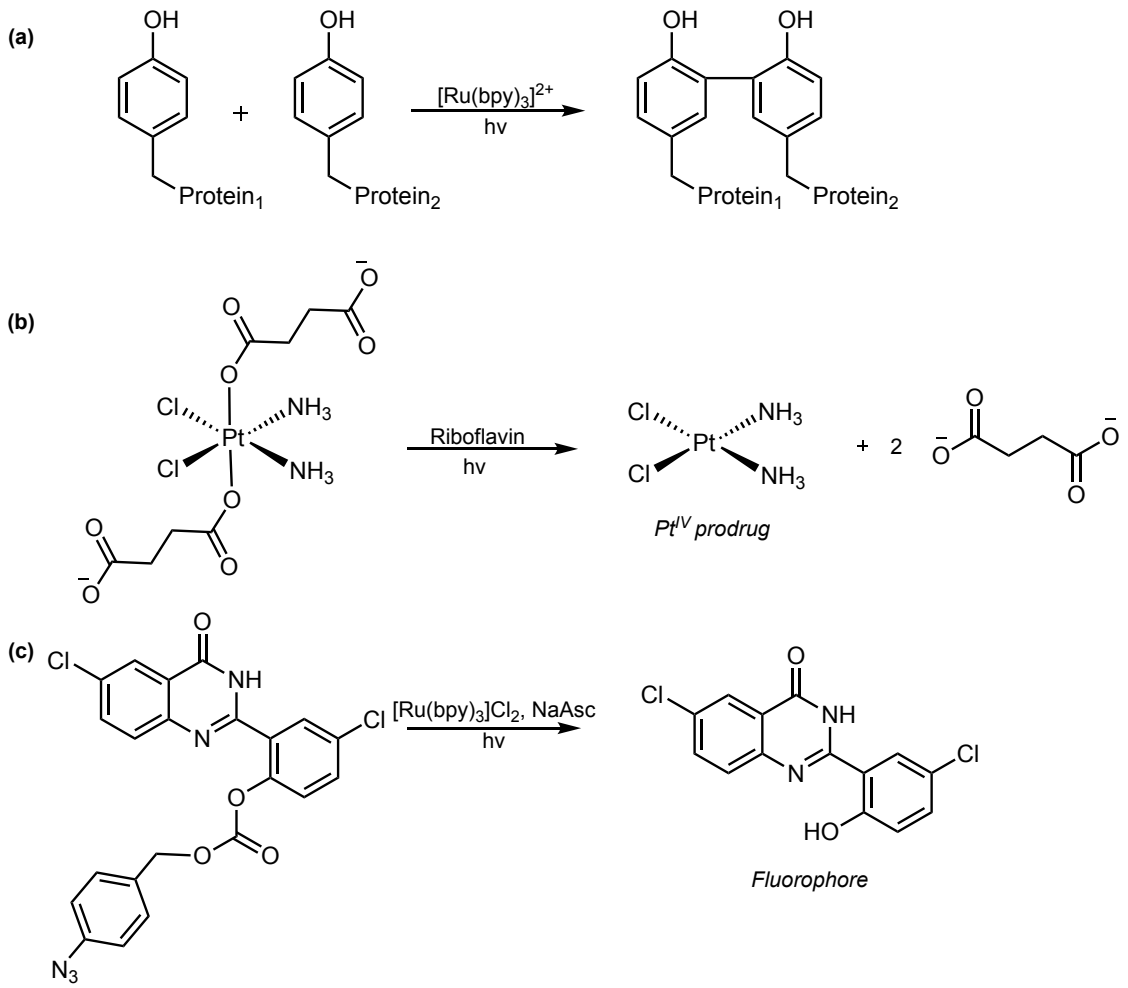

Figure 11 Some examples of bioorthogonal photocatalysis. a) Example of protein dimerization through ligation of tyrosines. b) Releasing of Pt ^{IV} prodrug; c) Releasing of a fluorophore for bioimaging.

The idea behind this project is to explore the viability of achieving visible light initiated photocatalyzed processes in biological media.

1.2.4. Photocatalysts: organic dyes and transition-metal complexes

In visible-light-induced redox transformations it is crucial to choose an adequate catalyst with a high absorptivity coefficient in the visible region of the spectra and a long lifetime excited state as well as a suitable redox potential.

Organic dyes are chromophores with a high absorption coefficient in the visible region. Their capacity to undergo electron and energy transfer processes after being excited have extended their use as catalysts. In addition, they avoid the use of toxic-metallic complexes, and they are usually cheaper.

However, transition-metal complexes show unique redox properties and several examples have been described for ruthenium (II)/iridium (III) polypyridyl complexes, cobalt and palladium species. Especially remarkable are ruthenium polypyridyl complexes and, in particular, $[Ru(bpy)_3](PF_6)_2$ satisfies the above conditions: the wavelength for maximum absorbance is 452 nm (visible-near UV region) allowing the reaction to be performed in biological media.

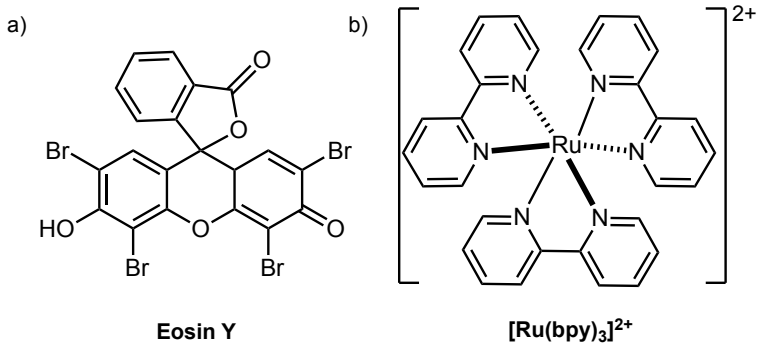

Figure 12 a) Eosin Y as an example of organic dye. b) $[Ru(bpy)_3]^{2+}$ as an example of transition-metal complex.

After absorption of a photon, electron transfer from t_{2g} ruthenium orbital to π^* ligand orbital takes place, resulting in a long lifetime excited state (1100 ns) that triggers electron or energy transfer processes. As a result, excited-state catalyst can lead to radical formation from different substrates and gives a new approach to radical chemistry, traditionally dependent on powerful radical initiators (AIBN, Bu_3SnH…) and high temperatures.

Finally, taking into account the biocompatible excitation wavelength and solubility in water of $[Ru(bpy)_3](PF_6)_2$, combination of both constitutes an environmentally friendly method to access free radical intermediates. In this sense, diazonium salts are suitable oxidative quenchers in photoredox chemistry and there are several examples in literature supporting their use as nice precursors of radicals obtained by electron transfer processes triggered by these catalysts. [26; 27]

1.2.5. Substrates: aryldiazonium salts

Diazonium salts, in particular those derived from anilines, are inexpensive and versatile compounds appropriated for loads of synthetic routes in organic chemistry. Aryldiazonium salts are suitable precursors for transformations in water as they are commonly soluble and highly reactive. Mainly, aryldiazonium salts can easily undergo two types of reactions: nitrogen-removal or nitrogen-retention processes. [28]

On one hand, the driving force of the first type of chemistry is the release of N_2 from the aryldiazonium substrate. This ability has turned them into highly suitable precursors for Meerwein-type alkene functionalization or Sandmeyer-type reactions for C-S, C-P and C-B bond formation. On the other hand, concerning the nitrogen-retention processes, aryldiazonium salts act as electrophiles in N-N bond forming transformations or as radical acceptors in radical addition reactions. [28]

On these grounds, this project is focused on N_2 releasing reactions that result in aryl radical formation in presence of a redox-active transition-metal complex after irradiation with light. Even though many diazonium salts can be directly photolyzed, UV photons are needed. Therefore, photoredox catalysts are used to sensitize these organic molecules through electron or energy transfer processes. Under these conditions, aryldiazonium salts are able to take up an electron from the catalyst and the energy required for the redox reaction to proceed is provided by light. The reaction takes place at room temperature and, as nitrogen is released, it does not interfere with the reaction mixture. Moreover, these transformations undergo through radical species and the chemoselectivity is high.

Overall, these salts are extremely useful for synthetic methodologies as they play a fundamental role in the transformation and functionalization of the aromatic carbon they are attached to, leading to different types of bond formation (C-H, C-C-, C-S, C-P…) and lots of different aromatic derivatives.

However, these compounds can be unstable. In fact, the stability of diazonium salts moves in a wide range from those that are explosive to those that are difficult to decompose. As a result, these salts can be really hard to isolate. Nevertheless, some of them are isolable, such as aryl diazonium tetrafluoroborate, tosylate, disulfonimide or carboxylate [29] and they are commonly storaged under special conditions, such as low temperatures (below 0 ^{o}C) or avoiding contact with light. The stability of these diazonium salts is subjected to the type and position of the substituents on the aromatic ring. The decomposition temperature of these chemicals can be determined by using differential scanning calorimetry (DSC) and in general, not many trends are observed. [29]

2. OBJECTIVES AND PLAN

2.1. Objective

As commented, even though photocatalytic methods are a valuable tool in synthesis, there are little examples of bioorthogonal photocatalytic strategies. The reason behind that might be the formation of highly reactive radical species that restrict the applications. Nevertheless, there are several examples of reactions in aqueous media.

The objective of this project is the design and evaluation of different photochemical transformations in aqueous media, and the viability of performing them in a bioorthogonal manner. For this purpose, intermolecular processes that encompass both C-C and C-heteroatom bond formation are chosen for the obtention of interesting structures, such as phenanthrenes, benzotiophenes or coumarins.

Moreover, to prove bioorthogonality and compatibility with biological media, the reactions will be tested in more complex media such as DMEM, BSA solution, lysates and finally in presence of HeLa cells.

Finally, preliminary experiments might be carried out in presence of living cells, consisting in the synthesis of a highly fluorescent product, an AIE fluorophore by means of a bioorthogonal photocatalytic reaction.

3. RESULTS AND DISCUSSION

3.1. Synthesis of phenanthrenes

In 2012, Zhou and co-workers reported the synthesis of mono- and di-substituted phenanthrenes by Eosin-Y catalyzed visible light induced [4+2] benzannulation.[26] In the present work, the reaction between biaryldiazonium tetrafluoroborate salt **3** and methyl propiolate **4** displayed in *figure 13* was chosen as a model reaction.

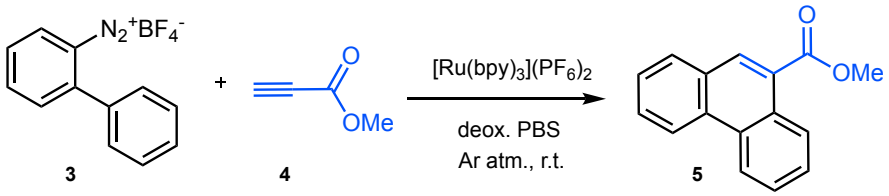

Figure 13 Reaction conditions for phenanthrene formation.

While the authors described the use of Eosin-Y in acetonitrile, preliminary results of the group led us to introduce two initial changes. On the one hand, $[Ru(bpy)_3](PF_6)_2$ was used instead of Eosin-Y. As mentioned in *section 1.2.4.*, the use of $[Ru(bpy)_3](PF_6)_2$ is preferred because of the solubility in aqueous media as well as biocompatible excitation wavelength and long-life excited state. On the other hand, deoxygenated PBS (saline phosphate buffer pH = 7.4) was selected as reaction media, which works as a first approximation to cellular media. In addition, to avoid degradation of the reactants, inert atmosphere was used.

Taking into account these aspects, for the experiments biaryldiazonium salt **3** (1 eq.) and $[Ru(bpy)_3](PF_6)_2$ were loaded inside a sealed vial under inert atmosphere. Then, PBS was added, followed by methyl propiolate **4** (5 eq.). The vial was introduced inside the photoreactor (for technical characteristics see *annex IV*) and was irradiated using blue LED lamp (*figure 14*). Once the reaction was completed, the crude was subjected to adequate work-up and the final product was isolated by flash column chromatography for characterization purposes (for further details see *annex II: 2.1.1.* and *annex III: 2.1.1*).

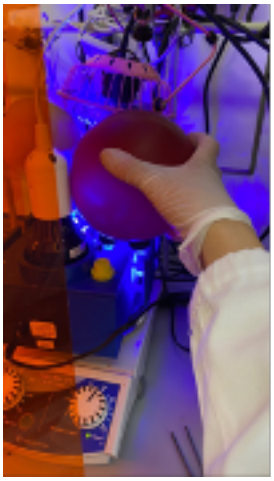

Figure 14 Set-up for photocatalyzed reactions.

The reaction mechanism proposed by the authors for phenanthrene formation is displayed in *figure 15,* taking into account the use of $[Ru(bpy)_3](PF_6)_2$ instead of Eosin-Y. As showed in the reaction scheme, reaction starts with excitation of ruthenium complex ($\lambda = 452\ nm$), followed by single electron transference to biaryldiazonium salt, resulting in biphenolic radical formation and releasing of N_2. This radical is added to the alkyne and cyclization affords phenanthrene structure. Finally, electron transference back to ruthenium complex, regenerates the catalyst and resulting carbocation recovers aromaticity after deprotonation.

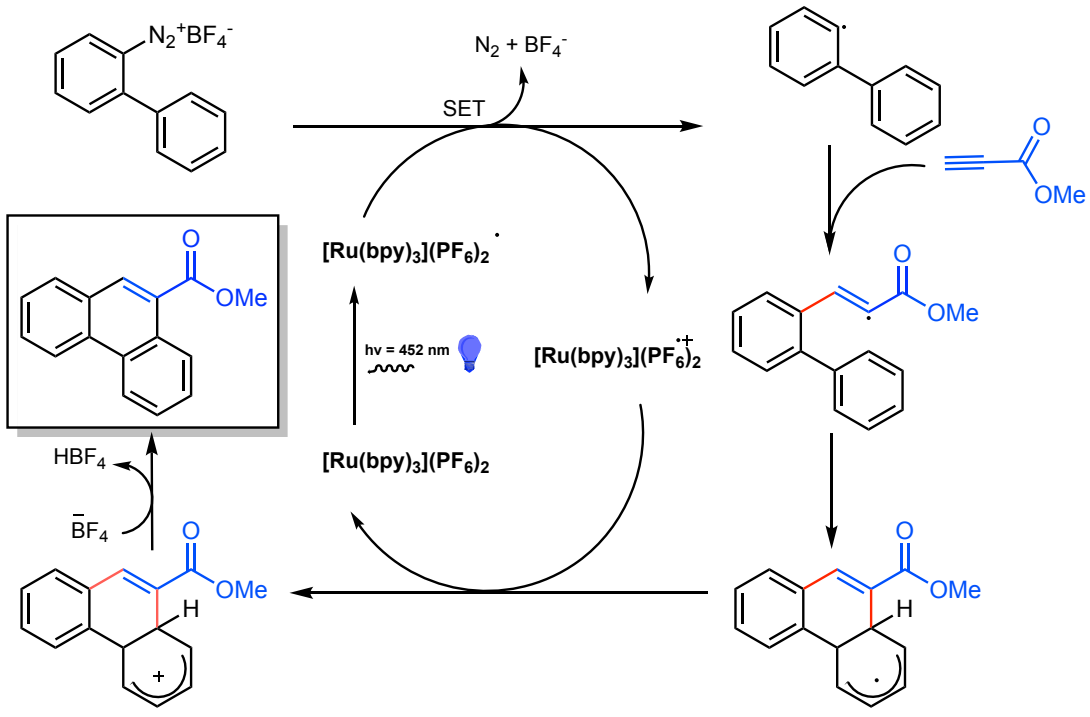

Figure 15 Reaction mechanism proposed by the authors adjusted to $[Ru(bpy)_3](PF_6)_2$. [26]

The reaction was optimized for the photocatalyzed synthesis of *methyl 9-phenanthrene carboxylate* **5**. In this case, for yield determination (*annex IV*), nitromethane in $CDCl_3$ was used as an internal standard.

In concrete, the relation between the signal for nitromethane (δ = 4.32 ppm) and that for the metoxi group (δ = 4.05 ppm) was calculated to get the yield as shown in *figure 16.* Moreover, two additional signals (8.9 ppm and 8.5 ppm) that ideally integrate by 1H could be used too, therefore yields were estimated as an average of the three values.

$$\%Yield = \frac{1.82/3 + 0.59 + 0.61}{3} x\ 100 = 60.2\%$$

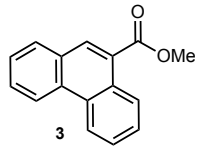

3

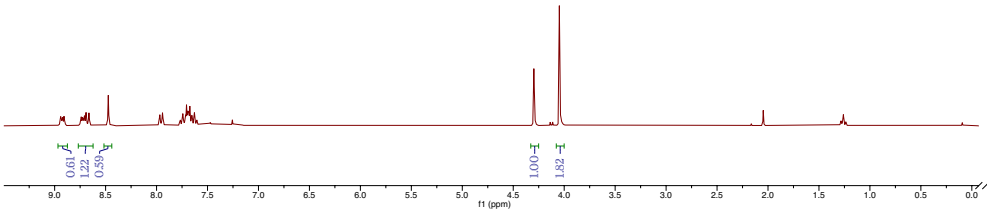

Figure 16 Example of yield's estimation for phenanthrene formation.

3.1.1. Optimization

First experiments were carried out with a concentration of biaryldiazonium salt **3** of 330 mM, and the reaction was evaluated after different irradiation times: 1, 5, 15, 30 min and 2, 6 and 24 h. The irradiation time refers to the time the samples are exposed to the LED lamp. In the following experiments, irradiation time is almost equal to the reaction time as samples were introduced inside the photoreactor just after addition of the reactants following the procedure described in *annex II* (*2.1.1.*).

The results obtained are displayed in *Table 1.* From them, it can be deduced that the changes made in the reaction conditions are compatible with phenanthrene formation. Moreover, these data can be used to get an idea of the kinetic profile of the reaction. In concrete, it can be observed that the reaction is fast, the result obtained for 5 min is more than double of the result obtained for 1 min, while the difference between the yield afforded by 15 and 30 min of irradiation is less than 10%. Indeed, after 6 h on, the yield afforded for phenanthrene formation remains constant.

*Table 1 Yields as a function of irradiation time for a concentration of diazonium salt **3** of 330 mM.*[a]

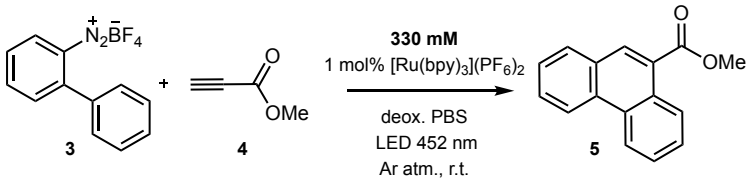

3 4 5

Entry	Time/ min	Yield%
1	1	18
2	5	38
3	15	38
4	30	43
5	120	53
6	360	62
7	1440	62

[a] Reaction conditions: **3** (0.2 mmol), **4** (1 mmol), $[Ru(bpy)_3](PF_6)_2$ (0.002 mmol) in deoxygenated PBS (0.6 mL), LED (452 nm), Ar atm. and r.t.

Then, experiments were repeated with a concentration of diazonium salt **3** of 10 mM and yield was again calculated after 1, 5, 15, 30 min as well as 2, 6 and 24 h of irradiation. The values obtained follow the same tendency as those for 330 mM. Nevertheless, dilution seems to favor the reaction as after 1 min of irradiation the yield is higher for 10 mM concentration. This fact can be explained taking into account the radical nature of the transformation: at shorter reaction times, when diluting, a lower amount of radicals is formed and side reactions are reduced (*Table 2*).

*Table 2 Yields as a function of irradiation time for a concentration of diazonium salt **3** of 10 mM.*[a]

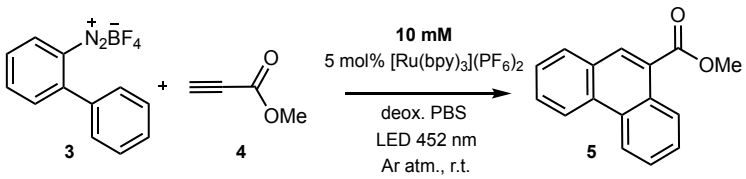

3 4 5

Entry	Time/ min	Yield %
1	1	40
2	5	40
3	15	41
4	30	44
5	120	45
6	360	45
7	1440	47

[a] Reaction conditions: **3** (0.05 mmol), **4** (0.025 mmol), $[Ru(bpy)_3](PF_6)_2$ (0.0025 mmol) in deoxygenated PBS (5.0 mL), LED (452 nm), Ar atm. and r.t.

However, it can be also observed that yields are maintained in time. In order to clarify the reason behind these hardly constant and moderate yields, two additional experiments were carried out. These essays consisted in adding to reaction media, after two hours of irradiation, either one equivalent of catalyst (*entry 2*) or one equivalent of diazonium salt **3** (*entry 3*). The samples were irradiated for two additional hours. Moreover, these experiments were performed in parallel to another irradiation experiment of 2 h in order to compare the results (*entry 1*).

Table 3 Yields obtained after diazonium salt addition (entry 2) and catalyst (entry 3).[a]

Entry	Addition of catalyst	Addition of salt 3	Time/min	Yield %
1	No	No	120	38
2	Yes	No	120 + 120	29
3	No	Yes	120 + 120	64

[a] Reaction conditions: **3** (0.05 mmol), **4** (0.025 mmol), $[Ru(bpy)_3](PF_6)_2$ (0.0025 mmol) in deoxygenated PBS (5.0 mL), LED (452 nm), Ar atm. and r.t for 2 h, followed by addition of **4** (0.025 mmol; entry 2) and of **3** (0.05 mmol; entry 3).

From these results, it can be observed that after addition of a new equivalent of substrate **3** and irradiation for two additional hours, yield is almost doubled (*entry 3*). This result suggests that the photocatalyst is still active and reaction stops after first two hours of irradiation due to photodegradation of the substrate. In addition, reduction of the yield in case of *entry 2*, suggests that not only the starting salt is being decomposed but also the product of the reaction.

Apart from product decomposition, in the crude of the reaction several additional aromatic signals were observed by NMR indicating the presence of side products that could not be isolated yet. The formation of these side products could also explain the moderate yields obtained.

At this point, in order to improve reaction yield, slow addition of diazonium salt was carried out. As this reaction implies the formation of radicals, species with an unpredictable behaviour and generally instable, it is thought that slow addition of the salt could enable a controlled formation of these radicals, resulting in an improvement of the yields.

In concrete, an automatic pump machine was used to continuously add a stock solution of diazonium salt **3** in PBS. The stock solution was prepared in accordance to annex II (*2.1.3*) and added to the sealed vial through a syringe, taking 5 minutes (addition rate: 0.04 mL/min) to complete the addition by using the pump (*figure 17*). The results obtained support the hypothesis and the yield calculated under these conditions increased to 61% (in contrast to 45% calculated without slow addition).

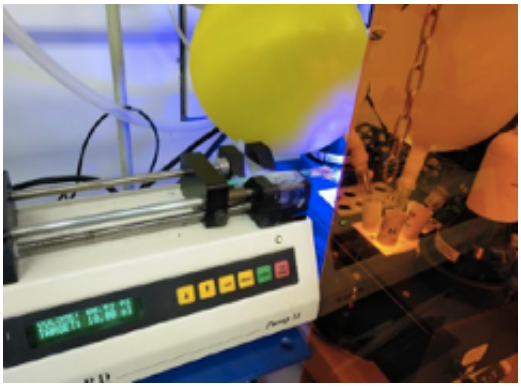

*Figure 17 Set-up for slow addition of diazonium salt **3**.*

3.1.2. Bioorthogonality

Encouraged by the results obtained with the slow addition of the diazonium salt, reaction was next carried out in more complex, biologically relevant media. With this objective, three different media were used: DMEM (cell culture media enriched with glucose and sodium pyruvate but no proteins, lipids or growth factors); BSA in PBS (5 mg/mL solution of bovine serum albumin protein in saline phosphate buffer); and cell lysates (1.03 mg/mL). Finally, in a fourth essay the reaction was carried out in presence of HeLa cells using PBS as reaction media (5 mg/mL).

Table 4 Yields obtained using more complex reaction media.

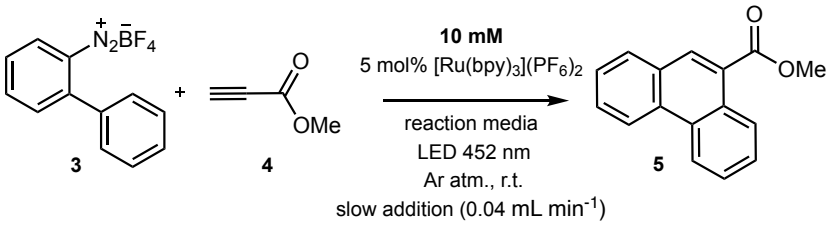

Entry	Reaction media	Time/h	Yield %
1	DMEM[a]	24	33
2	BSA in PBS[b]	24	30
3	Cell lysates[c]	24	27
4	HeLa cells in PBS[d]	24	16

[a] Reaction conditions: **3** (0.25 mmol), **4** (1.25 mmol), photocatalyst (0.0125 mmol) in DMEM(1.0 mL), LED (452 nm), Ar atm. and r.t. [b] Same conditions in BSA in PBS: 5 mg/mL; [c] Same conditions in cell lysates: 1.03 mg/mL. [d] Same conditions in presence of HeLa cells in PBS (5 mg/mL).

From these results, it can be confirmed that phenanthrene formation still takes place selectively in more complex biological media, which is somewhat similar to cells. Therefore, this transformation can be considered bioorthogonal. Nevertheless, yields are poor and the concentration of biaryldiazonium salt **3** used is still high. Consequently, there is much work to do in order to achieve phenanthrene formation in live settings in an efficient manner.

3.2. Synthesis of benzotiophenes

Benzotiophenes are a group of really useful compounds as many commercial drugs contain a benzotiophene core. Moreover, these molecules have also found applications in catalysis, materials science and biology, among other fields.

As a consequence, many methods have been developed for the synthesis of benzotiophenes, but they usually require the use of transition metals and harsh conditions. To overcome these issues, König and coworkers described the photoinduced synthesis of benzotiophenes through radical annulation of the analogue diazonium salt **6** using Eosin Y ($\lambda = 539\ nm$) as a catalyst (*figure 18*). [30]

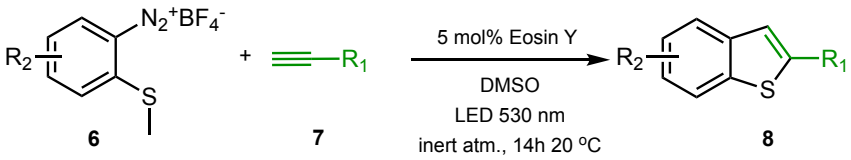

Figure 18 Reaction conditions for benzotiophene formation.

The plausible reaction mechanism is displayed in *figure 19*. First step is excitation of the organic dye ($\lambda = 539\ nm$), causing single electron transference to aryldiazonium salt, resulting in the pertinent radical and releasing of N_2. This radical is added to the alkyne and cyclization affords benzotiophene structure. Finally, electron transference back to Eosin Y regenerates the catalyst and removal of the methyl group by sulfoxide gives the final product.

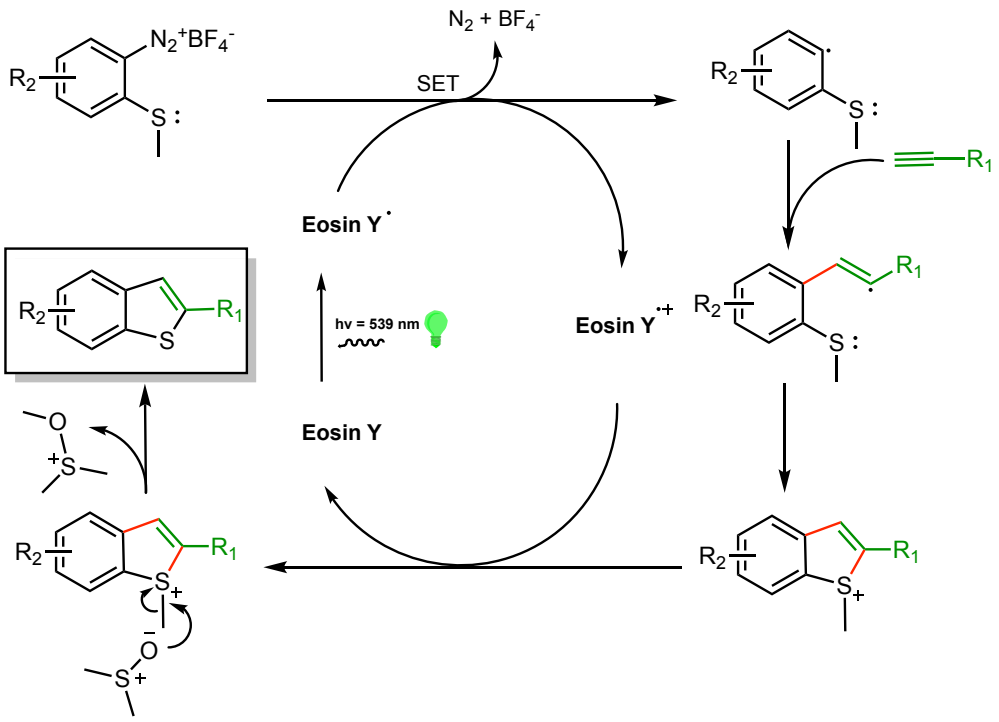

Figure 19 Reaction mechanism proposed by the authors. [30]

In concrete, the reaction between aryldiazonium salt **6a** (1 eq.) and phenylacetylene **7a** (5 eq.) catalysed by Eosin Y in DMSO was first tested. Moreover, the concentration of **6a** used was 250 mM and the experimental protocol is described in detail in annex II (*2.2.1*). Fortunately, the product **8a** was obtained after 14 h of irradiation and characterized after isolation by ^{1}H-NMR (*annex III: 2.2.1*).

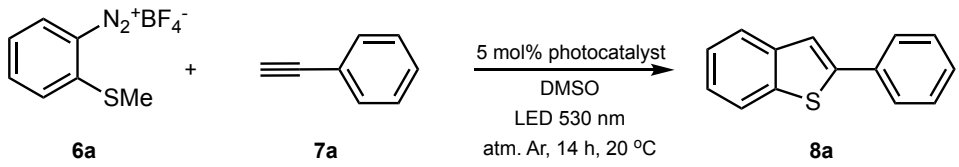

*Figure 20 Scheme of the reaction using aryldiazonium salt **6a** and alkyne **7a**.*

However, the yield obtained after isolation was really poor (16%), probably due to product decomposition. The reaction was repeated using an internal standard, as it allows to monitor the reaction and calculate the yield, by using it in combination with NMR spectroscopy. This methodology can be used as long as the product has a singular and isolated signal, but for product **6a** all the signals were aromatic and they were all really close (*annex III: 2.2.1.*).

As it was needed to introduce a characteristic signal in the NMR spectra of the product, it was considered the idea of introducing a metoxi group in one of the reagents, as it would give an aliphatic and isolated signal. In concrete, it was important to introduce it in the limiting reagent (e.g. aryldiazonium tetrafluoroborate salt), otherwise it would remain after completion of the reaction, preventing the yield to be determined properly.

Therefore, the next step consisted in trying to perform the reaction using aryldiazonium salt **6b**, synthesized from *p*-anisidine (following protocols *1.1.2.* and *1.2.2.* described in *annex II*). As it is displayed in *figure 21*, all the other reaction conditions (alkyne, catalyst, irradiation time, temperature, concentration…) were maintained.

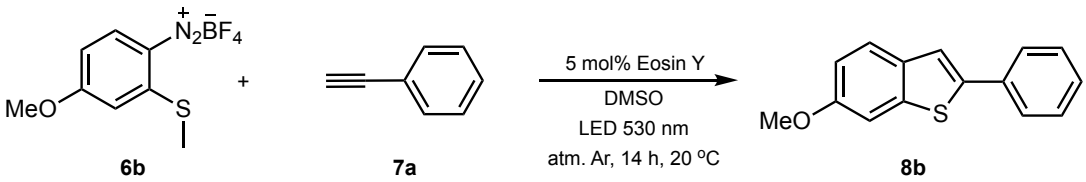

*Figure 21 Scheme of the reaction using aryldiazonium salt **6b** and alkyne **7a**.*

Gratifyingly, product **6b** was obtained by following the protocol described in annex II (*2.2.1.*) , isolated by flash column chromatography in 37% yield and characterized by ^{1}H-NMR (*annex III: 2.2.2.*).

As for phenanthrenes, in order to determine the yield (*annex IV*), nitromethane in $CDCl_3$ was used as an internal standard. In concrete, the relation between the signal for nitromethane (δ = 4.32 ppm) and that for the metoxi group (δ = 3.89 ppm) was calculated to get the yield as shown in *figure 22*.

$$\%Yield = \left(\frac{1.12}{3}\right) x\ 100 = 37.3\%$$

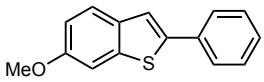

6b

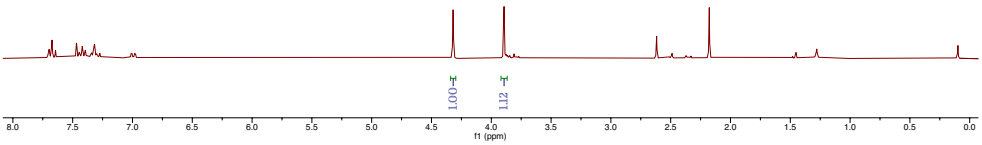

Figure 22 Example of yield's estimation for benzotiophene formation.

3.2.1. Optimization

In order to turn reaction conditions into more biocompatible, several changes were introduced, starting with the reaction media. In concrete, first attempts were focussed on checking the compatibility of the reaction with aqueous media (e.g. deoxygenated PBS). With this purpose, the reaction was performed in PBS, keeping all the other reaction conditions (catalyst, irradiation time, temperature, concentration…).

*Table 5 Yield obtained for the synthesis of benzotiophene **6b** as a function of reaction media and photocatalyst.[a]*

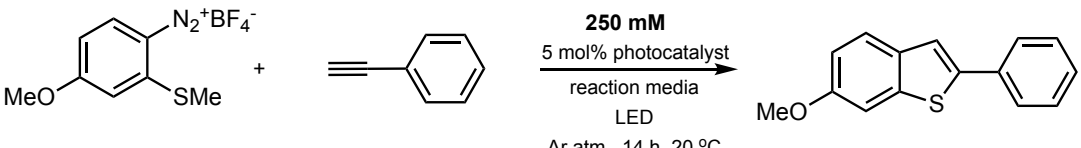

6b **7a** **8b**

Entry	Reaction media	Photocatalyst	Yield %
1	DMSO	Eosin Y	34
2	PBS	Eosin Y	45
3	PBS	$[Ru(bpy)_3](PF_6)_2$	26

[a] Reaction conditions: **6a** (0.25 mmol), **7a** (1.25 mmol), photocatalyst (0.0125 mmol) in the different reaction media (1.0 mL), LED (452 nm), Ar atm. and r.t.

Gratifyingly, the yield is even improved when using PBS as reaction media (*Table 5*). Encouraged by the results, the following step, consisted in using different catalysts to compare their behaviour for the synthesis of benzotiophenes. In concrete, the reaction using either Eosin Y or $[Ru(bpy)_3](PF_6)_2$ was carried out and the yields were determined, as shown in *Table 5*.

As better results were obtained using Eosin Y in PBS, next step implied the comparison between different catalyst loadings, keeping all reaction conditions used before. The yield afforded by the different catalytic loadings is shown in *Table 6*.

Table 6 Yields obtained for benzotiophene formation as a function of catalyst loading. [a]

Entry	Catalyst loading %	Yield %
1	5%	45
2	7.5%	42
3	10%	40

[a]Reaction conditions: **6a** (0.25 mmol), **7a** (1.25 mmol), photocatalyst (0.0125 mmol) in the different reaction media (1.0 mL), LED (452 nm), Ar atm. and r.t.

From the obtained results, it can be deduced that 5% catalyst loading affords the highest yield. However, the yield obtained is still low and further experiments must be performed.

3.3. Synthesis of coumarins

In this case, the starting point is the photoinduced synthesis of 3-difluoroacetylated coumarins described by Baoming and coworkers in 2015. The authors reported as the highest-yielded the transformation of phenyl alkynoate derivatives and ethyl-2-bromo-2,2-difluoroacetate into the desired coumarin after photoexcitation of $[fac\text{-}Ir(ppy)_3]$ in DMF and in presence of K_2CO_3 as a base. [(31)]

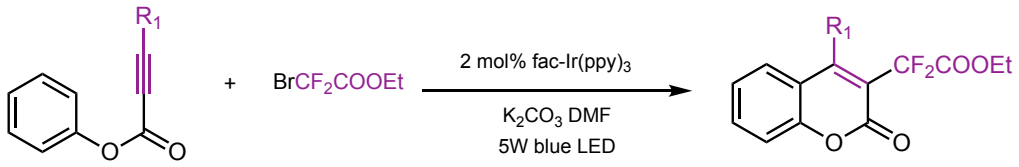

Figure 23 Reaction conditions reported by Baoming et al. [31]

However, inspired on the previous experiences using diazonium salts as source of radicals, it was hypothesized that these versatile substrates could be used to participate in the formation of coumarins. The use of different photocatalysts was considered as well. Therefore, the mechanism shown in *figure 24* is adjusted to the use of any aryldiazonium salt and any photocatalyst (commonly Eosin Y or $[Ru(bpy)_3]^{2+}$).

The plausible reaction mechanism is similar to that for phenanthrenes and benzotiophenes, but in this case, intermolecular $C(sp^2)$-$C(sp^2)$ bond formation is followed by intramolecular cyclization of the alkyne structure to afford the skeleton of coumarins.

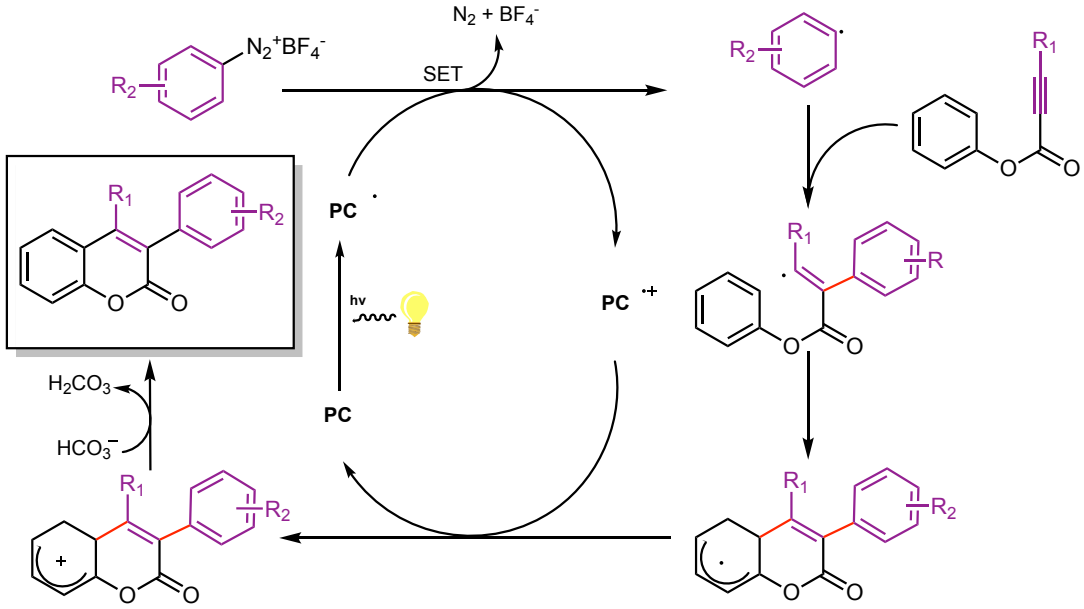

Figure 24 Reaction mechanism proposed by the authors and adjusted to any aryldiazonium salt and photocatalyst (PC). [31]

Particularly, *p*-metoxi aryldiazonium tetrafluoroborate salt **10** was used in order to enable the monitorization of the reaction by NMR-spectroscopy with internal standard

as this metoxi substituent would hopefully give an isolated signal in the aliphatic region of the spectra.

Moreover, first experiments were focused on using **9** synthesized from phenol as described in annex II (*1.3.1*). The reason behind is the fluorescence product **11** might show that would allow to follow the reaction inside cells in future experiments. As this transformation has not been previously described, different catalysts and reaction media were scanned, as well as the presence or absence of base. In general, the reaction conditions are summarized in *figure 25*.

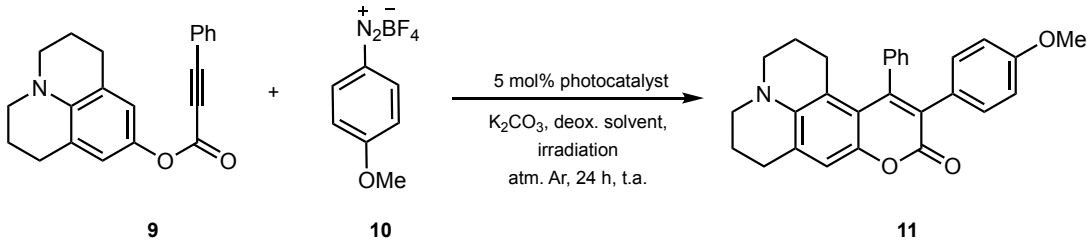

9 **10** **11**

Figure 25 Resumed reaction conditions for coumarin formation.

Unfortunately, none of the combinations enabled the identification of the product. Even though the reaction was followed by TLC (thin layer chromatography) and consumption of the starting reactants was observed, the crude consisted in a complex mixture of products from which the desired product could not have been isolated and characterized yet.

3.4. Reactions to be explored in cells

The final purpose of the project was to perform light-induced photocatalytic reactions inside living cells. This requires the production of a fluorescent compound in order to follow the reaction in real time by using fluorescence microscopy. However, neither phenanthrene nor benzotiophene derivatives prepared before were fluorescent. Therefore, a new transformation, which gives fluorescent compound **14** was proposed.

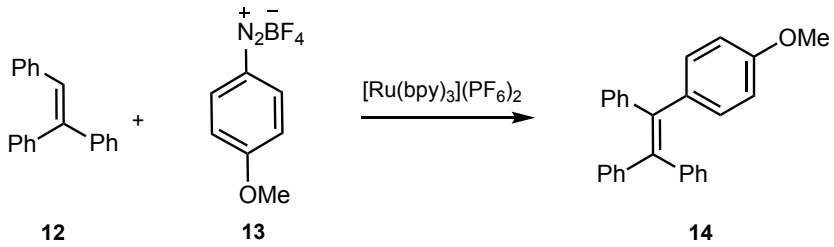

Figure 26 Scheme of reaction for the synthesis of AIE fluorophore.

As preliminary examples on the viability of this transformation had been developed in the group, it was checked if it would be possible to perform the process in the presence of living cells.

In concrete, HeLa cells were treated with the photocatalyst [Ru] during 30 minutes before being washed with DMEM to remove extracellular [Ru]. Then, they were incubated with substrates **12** and **13** for 30 minutes before irradiation with blue light (λ = 460 nm) for 10 minutes (for detailed procedure see *annex II 2.4.*). Additionally, two control experiments were carried out consisting in incubation for 30 minutes of 50 µM [Ru] and 100 µM of substrates **12** and **13.** Finally, the following micrographies shown in *figure 27* were taken.

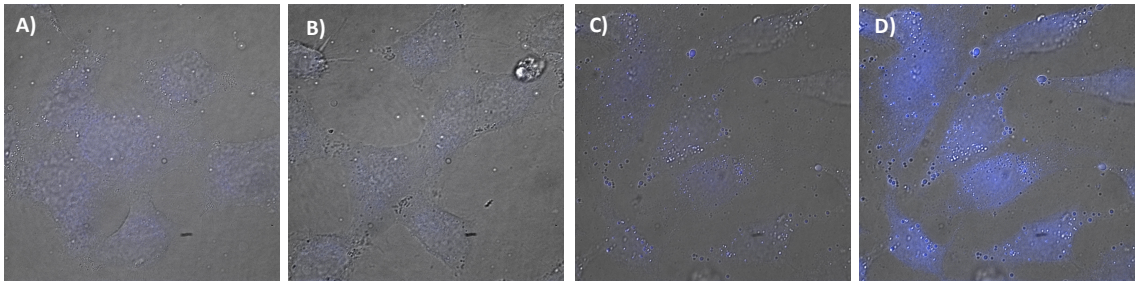

Figure 27 Bioorthogonal photocatalytic reaction inside HeLa cells. Fluorescence micrographies (brightfield) after incubation with: ***(a)*** *substrates* ***12*** *and* ***13; (b)*** *[Ru];* ***(c)*** *[Ru], washing step, substrates* ***12*** *and* ***13****;* ***(d)*** *same as* ***(c)*** *but 10 min of irradiation at λ = 460 nm. Blue channel: I_{exc} = 385 nm I_{em} = 410-480 nm.*

From the comparison of the fourth, it can be concluded that there is not an observable intracellular fluorescence in the case of control experiments **(a)** and **(b)**. In panel **(c)**, without irradiation, no intracellular staining is observed, while there is an increase of blue fluorescence for experiments **(d)** corresponding with the intracellular formation of the product after irradiation.

The results are very promising but very preliminar since this part of the project has been recently initiated and it must be exhaustively studied.

CONCLUSIONS

The experimental work of this project consisted in the study of different photoinduced reactions in aqueous media and in presence of biologically relevant solvents. The intermolecular processes explored encompass both C-C and C-heteroatom bond formation for the obtention of interesting structures, such as phenanthrenes, benzotiophenes or coumarins.

The synthesis of phenanthrenes was studied, optimizing reaction conditions using ruthenium complex in PBS by using different techniques such as slow addition methods. Moreover, the reaction was successfully performed in different biological media, such as DMEM, BSA solution, cell lysates and even in presence of HeLa cells. Regarding the synthesis of benzotiophenes, the compatibility of the system with more complex media (e.g., PBS) was explored comparing the activity of different catalysts as preliminary studies needed to achieve bioorthogonality. However, in relation to the synthesis of coumarins, the desired product could not be isolated.

Finally, preliminary experiments carried out in living cells for the synthesis of an AIE fluorophore showed that the transformation can occur.

CONCLUSIONES

El trabajo experimental en este proyecto consistió en el estudio de diferentes reacciones fotoinducidas en medio acuoso y en la presencia de disolventes biológicos. Los procesos intermoleculares estudiados incluyen la formación de enlaces C-C y C-heteroátomo para la obtención de estructuras interesantes como los fenantrenos, benzotiofenos y cumarinas.

La síntesis de fenantrenos se ha estudiado, optimizando las condiciones de reacción empleando el complejo de rutenio en PBS y utilizando diferentes técnicas como los métodos de adición lenta. Así mismo, la reacción se llevó a cabo en diferentes medios biológicos, como DEMEM, solución de BSA, lisados celulares e incluso en presencia de

células HeLa. Respecto a la síntesis de benzotiofenos, se ha explorado la compatibilidad del sistema con medios más complejos (por ejemplo PBS), comparando la actividad de diferentes catalizadores y cargas catalíticas, como estudios preliminares necesarios para alcanzar la bioortogonalidad del proceso. Sin embargo, en relación a la síntesis de cumarinas, el producto deseado no se ha podido aislar.

Finalmente, los experimentos preliminares llevados a cabo en células vivas para la síntesis de un AIE fluoróforo muestran que la transformación se puede llevar a cabo.

CONCLUSIÓNS

O traballo experimental neste proxecto consistiu no estudo de diferentes reaccións fotoinducidas en medio acuoso e na presencia de disolventes biolóxicos. Os procesos intermoleculares estudiados inclúen a formación de enlaces C-C e C-heteroátomo para a obtención de estruturas interesantes como fenantrenos, benzotiofenos e cumarinas.

A síntese de fenantrenos someteuse a estudo, optimizando as condicións de reacción, empregando o complexo de rutenio en PBS e utilizando diferentes técnicas como os métodos de adición lenta. Asimesmo, a reacción se levouse a cabo en diferentes medios biolóxicos, como DEMEM, solución de BSA, lisados celulares e incluso en presencia de células HeLa.

Respecto da síntese de benzotiofenos, explorouse a compatibilidade do sistema con medios más complexos (por exemplo PBS), comparando a actividade de diferentes catalizadores e cargas catalíticas, como estudios preliminares necesarios para alcanzar a bioortogonalidade do proceso. Non obstante, en relación a síntese de cumarinas, o produto desexado non puido illarse.

Finalmente, os experimentos preliminares levados a cabo en células vivas para a síntese dun AIE fluoróforo mostran que a transformación pode levarse a cabo.

References

1. Scinto, S. L.; Bilodeau, D. A.; Hincapie, R.; Lee, W.; Nguyen, S. S.; Xu, M.; Ende, C. W.; Finn, M. G.; Lang, K.; Lin, Q.; Pezaki, J. P.; Prescher, J. A.; Robillard, M. S. and Fox, J. M. (2021). Bioorthogonal chemistry. *Nat. Rev. Methods Primers*, **1 (30)**.

2. Alonso-de Castro, S.; Ruggiero, E.; Ruiz-de-Angulo, A.; Rezabal, E.; Mareque-Rivas, J. C.; Lopez, X.; López-Gallego, F. and Salassa, L. (2017). Riboflavin as a bioorthogonal photocatalyst for the activation of a Pt^{IV} prodrug. *Chem. Sci.*, **8 (6)**, 4619-4625.

3. Wang, J.; Wang, X.; Fan, X. and Chen, P. R. (2021). Unleashing the power of bond cleavage chemistry in living systems. *ACS Cent. Sci.*, **7 (6)**, 929-943.

4. Vornholt, T.; Christoffel, F.; Pellizzoni, M. M.; Panke, S.; Ward, T. R. and Jeschek, M. (2021). Systematic engineering of artificial metalloenzymes for new-to-nature reactions. *Science Advances*, **7**, eabe4208.

5. Davis, H. J. and Ward, T. R. (2019). Artificial metalloenzymes: Challenges and opportunities. *ACS Cent. Sci.*, **5**, 1120-1136.

6. Vidal, C.; Tomás-Gamasa, M.; Destito, P.; López, F. and Mascareñas, J. L. (2018). Concurrent and orthogonal gold (I) and ruthenium (II) catalysis inside living cells. *Nat. Commun.*, **9 (1913)**.

7. Vidal, C.; Tomás-Gamasa, M.; Gutiérrez-González, A. and Mascareñas, J. L. (2019). Ruthenium-catalyzed redox isomerizations inside living cells. *J. Am. Chem. Soc.*, **141 (13)**, 5125-5129.

8. Fu, H. and Li, Y. (2020). Bioorthogonal ligations and cleavages in chemical biology. *ChemistryOpen*, **9 (8)**, 835-853.

9. Chalker, J. M.; Wood, C. S. C. and Davis, B. G. (2009). A convenient catalyst for aqueous and protein Suzuki-Miyaura cross-coupling. *J. Am. Chem. Soc.*, **131 (45)**, 16346-16347.

10. Li, N.; Lim, R. K. V.; Edwardraja, S. and Lin, Q. (2011). Copper-free Sonogashira cross-coupling for functionalization of alkyne-encoded proteins in aqueous medium and in bacterial cells. *J. Am. Chem. Soc*., **133 (39)**, 15316-15319.

11. Lin, Y. A.; Boutureira, O.; Lercher, L.; Bhushan, B.; Paton, R. S. and Davis, B. G. (2013). Rapid cross-metathesis for reversible protein modifications via chemical access to Se-allyl-selenocysteine in proteins. *J. Am. Chem. Soc*., **135 (33)**, 12156-12159.

12. Dommenholt, J.; Schmidt, S.; Temming, R.; Hendriks, L. J.; Rutjes, F. P.; van Hest, J. C.; Lefeber, D. J.; Friedl, P. and van Delft F.L . (2010). Readily accessible bicyclononynes for bioorthogonal labeling and three-dimensional imaging of living cells. *Angew. Chem. Int. Ed.*, **49 (49)**, 9422-9425.

13. Song, W.; Wang, Y.; Qu, J.; Madden, M. M. and Lin, Q. (2008). A photoinducible 1,3-dipolar cycloaddition reaction for rapid, selective modification of tetrazole-containing proteins. *Angew. Chem. Int. Ed.,* **47 (15)**, 2832-2835.

14. An, P.; Levandowski, T. M.; Erbay, T.G.; Liu, P. and Lin, Q. (2018). Sterically shielded, stabilized nitrile for rapid bioorthogonal protein labeling in live cells. *J. Am. Chem. Soc.*, **140 (14)**, 4860-4868.

15. Li, J.; Kong, H.; Huang, L.; Cheng, B.; Qin, K.; Zheng, M.; Yan, Z and Zhang, Y. (2018). Visible light-initiated bioorthogonal photoclick cycloaddition. *J. Am. Chem. Soc.*, **140 (44)**, 14542-14546.

16. Aonbangkhen, C.; Zhang, H.; Wu, D. Z.; Lampson, M. A. and Chenoweth, D. M. (2018). Reversible control of protein localization in living cells using a photocaged-photocleavable chemical dimerizer. *J. Am. Chem. Soc.*, **140 (38)**, 11926-11930.

17. Yiyun, C. (2020). *Illuminating biology with visible-light-induced biocompatible reactions. ChemPhotoChem*, **4 (5)**, 319-320.

18. Sun, K.; Lv, Q.-Y.; Chen, X.-L.; Qu, L.-B. and Yu, B. (2021). Recent advances in visible light mediated organic transformations in water. *Green Chem*., **23 (1)**, 232-248.

19. Fairbanks, B. D.; Macdougall, L. J.; Mavila, S.; Sinha, J.; Kirkpatrick, B. E.; Anseth, K. S. and Bowman, C. N. (2021).Photoclick chemistry: a bright idea. *Chem. Rev.*, **121 (12)**, 6915-6990.

20. Ryu, K. A.; Kaszuba, C. M.; Bissonnette, N. B; Oslund, R. C. and Olugbeminiyi, O. F. (2021). Interrogating biological systems using visible-light-powdered catalysis. *Nat. Rev. Chem.*, **5**, 322-337.

21. Xue, D.; Jia, Z.-H.; Zhao, C.-J.; Zhang, Y.-Y.; Wang, C. and Xiao, J. (2014). Direct arylation of N-heteroarenes with aryldiazonium salts by photoredox catalysis in water. *Chem. Eur. J*., **20 (10)**, 2960-2965.

22. Zou, L.; Li, P.; Wang, B. and Wang, L. (2019). Visible-light induced radical cyclization of N-allylbenzamides with CF_3SO_2Na trifluoromethylated dihydroisoquinolines in water at room temperature. *Green Chem.*, **21 (12)**, 3362-3369.

23. Das, S.; Ray, S.; Ghosh, A. B.; Samanta, P. K.; Samanta, S.; Adhikary, B. and Biswas, P. (2018). Visible light driven amide synthesis in water at room temperature from thioacid and amine using CdS nanoparticles as heterogeneous photocatalyst. *Appl. Organometal. Chem.*, **32 (3)**, 4199-4209.

24. Kodadek, T.; Duroux-Richard, I. and Bonnafous, J. (2005). Techniques: oxidative cross-linking as an emergent tool for the analysis of receptor mediated signaling events. *Trends in pharmacological sciences*, **26 (4)**, 210-217.

25. Sadhu, K. K.; Lindberg, E. and Winssinger, N. (2015). In cellulo protein labeling with Ru-conjugate for luminescence imaging and bioorthogonal photocatalysis. *Chem. Commun.*, **51 (93)**, 16664-16666.

26. Xiao, T.; Dong, X.; Tang, Y. and Zhou, L. (2012). Phenanthrene synthesis by eosin-Y-catalyzed visible light induced [4+2] benzannulation of biaryldiazonium salts with alkynes. *Adv. Synth. Catal*., **354 (17)**, 3195-3199.

27. Youn, S. W. and Lee, E. M. (2016). Metal-free-one-pot synthesis of N,N'-diarylamidines and N-arylbenzimidazoles from arenediazonium salts, nitriles and free anilines. *Org. Lett*., **18 (21)**, 5728-5731.

28. Wang, M.; Tang, B.-C.; Xiang, J.-C.; Chen, X.-L.; Ma, J.-T.; Wu, Y.-D. and Wu, A.-X. (2019). Aryldiazonium salts serve as a dual synthon: construction of fully substituted pyrazoles via rongalite-mediated three-component radical annulation reaction. *Org. Lett.*, **21 (22**), 8934-8937.

29. Schotten, C.; Leprevost, S. K.; Young, L. M.; Hughes, C. E.; Harris, K. D. M. and Browne, D. L. (2020). Comparison of the thermal stabilities of diazonium salts and their corresponding triazenes. *Org. Process Res. Dev.*, **24 (10)**, 2336-2341.

30. Hari, D. P.; Hering, T. and König, B. (2012). Visible light photocatalytic synthesis of benzotiophenes. *Org. Lett.*, **4 (20)**, 5334-5337.

31. Fu, W.; Zhu, M.; Zou, G.; C., Xu; Wang, Z. and Ji, B. (2015). Visible-light mediated radical aryldifluoroacetylation of alkynes with ethyl bromodifluoroacetate for the synthesis of 3-difluoroacetylated coumarins. *Org. Chem.*, **80 (9)**, 4776-4770.

ANNEX I

1. GENERAL INFORMATION

1.1. General information for chemical experiments:

Synthetic procedures are performed in round flasks. The solvents for organic synthesis are of reagent grade unless otherwise noted. Dry solvents are directly purchased from Aldrich and used without further purification. Chemicals are purchased from Sigma Aldrich, Alfa Aesar, Fluka or Acros Organics and used without further purification.

Reaction mixtures are stirred using Teflon-coated magnetic stir bars. The abbreviation ''r.t.'' refers to reactions carried out approximately at 23 ^{o}C. Temperature was kept using Thermowatch-controlled heating blocks.

Thin layer chromatography (TLC) is performed on Merck 60 (silica gel F_{254}) plates and components are visualized by observation under UV. Chromatographic purification of products is accomplished using flash column chromatography on Merck Geduran Si 60 (40-63 µm) silica gel (normal phase). Concentration is referred to the removal of volatile solvents via distillation using a rotary evaporator *Büchi R-210* equipped with a thermostated bath *B-491*, a vacuum regulator *V-850*, and a vacuum pump V-700, followed by residual solvent removal under high vacuum. Dryings were performed with anhydrous $MgSO_4$.

^{1}H NMR (300 MHz) spectra are recorded at room temperature on a *Varian Mercury* 300 MHz spectrometer and *Agilent VNMRS-300* spectrometer. The spectra are calibrated to the residual solvent peak, if possible. Multiplicities are abbreviated as follows: s = singlet, d = doublet, t = triplet, q = quartet, dd= doublet of doublets, td = triplet of doublets, m = multiplet, br = broad, bs = broad singlet. The chemical shifts for protons (δ) are reported in parts per million downfield from tetramethylsilane and are referenced to residual protium in the NMR solvent ($CDCl_3$ δ = 7.26 or DMSO δ = 2.500).

The coupling constants are given in (*J*) in Hz. NMR spectra are analysed using *MestreNova© NMR* data processing software (www.mestrelab.com).

Electrospray Ionization Mass Spectrometry (ESI/MS) was performed with a *Bruker Amazon IT/MS* coupled to an HPLC.

1.2. General information for biological experiments:

- **General executions and substances:** all steps are performed on a sterile clean bench *Telstar AV-100* at room temperature. Solutions stored in a fridge are warmed beforehand in a water bath (37 °C). Unless otherwise specified, all incubations are performed in DMEM.

- **Cell Culture:** All cell lines are cultured in DMEM (Dulbecco´s modified Eagle´s medium) containing 5 mM glutamine, penicillin (100 units/mL) and streptomycin (100 units/mL) (all from *Invitrogen*). Proliferating cultures are maintained in a 5% CO_2 humidified incubator at 37 °C.For all the experiments, cells are seeded in the corresponding well at the indicated concentration two days before treatment.

- **Fluorescence microscopy:** All images are obtained with an *Andor Zyla* mounted on a *Nikon TiE*. Confocal images are acquired in an *Andor Dragonfly* High Speed Confocal Platform. Images are further processed with *Image J* or *NIS* software (*Nikon*).

- **Microscopy settings:** The filter sets for the irradiation of the samples and the observation of the fluorescence of the products are as follows:

  For the Nikon (Semrock): filter cube Pyr: BP 376/30 nm, LP 460/50 nm and DM 425 nm; filter cube FITC-3540C-000: BP 482/35 nm, LP 536/40 nm and DM 506 nm; filter cube TRITC-B-000: BP 543/22 nm, LP 593/40 nm and DM 562 nm.

  LED 460 nm
  Field of irradiation: 15013.60 um^2
  Irradiation power: 250 mW.
  Power / surface: 16.651,56 mW/cm^2

- **Probes:** All probes have been previously synthesized and used in routinary cell experiments in the group.

ANNEX II

1. SYNTHESIS OF SUBSTRATES

1.1. Synthesis of aniline derivatives:

*1.1.1. Synthesis of 2-(methylthio)aniline (**1**)*

Compound **1** is prepared according to procedure described by Ray et al. and spectroscopic data are in agreement with the reported values. [1]

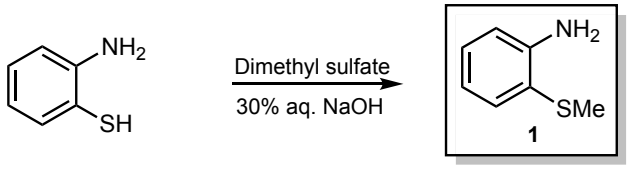

Figure 1 Reaction scheme for 2-(metylthio)aniline 1.

2- (Metylthio)aniline is synthesized from 2-aminotiophenol (1.0 mL, 10.0 mmol, 1 eq.) by adding it dropwise into an aqueous 30% NaOH solution (9.00 g in 30.0 mL) and treating it with dimethylsulfate (950.0 µL, 10.0 mmol, 1 eq.) while stirring at room temperature. The product is extracted with chloroform and isolated by flash column chromatography (hexane / ethyl acetate 6:4) as a gold oil in 71% yield.

R_f = 0.625 (hexane / ethyl acetate 4:1).

Yield = 71% (990.0 mg, 7.1 mmol).

^{1}H-NMR (300 MHz, $CDCl_3$): δ (ppm) 7.36 (dd, ^3J = 8.1, ^4J = 1.5 Hz, 1H), 7.10 (td, ^3J = 7.6, ^4J = 1.5 Hz, 1H), 6.78-6.68 (m, 2H), 4.29 (bs, 2H), 2.36 (s, 3H).

*1.1.2. Synthesis of 4-methoxy-2-(methylthio)aniline (**2**)*

Compound **2** is synthesized following the procedure described by König et al. and spectroscopic data are in agreement with the reported values. [2]

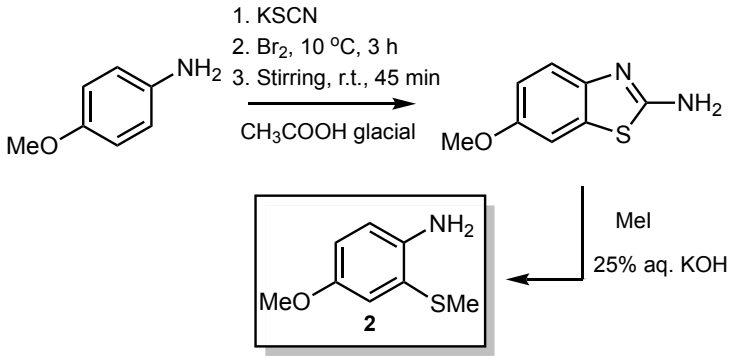

*Figure 2 Reaction scheme for 4-metoxi-2-(metylthio)aniline **2**.*

A mixture of *p*-anisidine (2.00 g, 16.3 mmol, 1 eq.) and KSCN (3.20 g, 32.6 mmol, 2 eq.) is dissolved in glacial acetic acid (27.5 mL) and cooled down until 10 °C. Then, a solution of Br_2 (1.6 mL, 32.6 mmol, 2 eq.) in glacial acetic acid (2.5 mL) is added dropwise and the resulting mixture is stirred for 3 h at 10 °C and for additionally 45 min at room temperature. The precipitate is filtered, redissolved in warm water and basified with saturated NaOH solution until pH = 8. Benzothiazole is obtained after filtration as a nude precipitate in 42% yield (1.20 g, 6.8 mmol).

Finally, benzothiazole (1.20 g, 6.8 mmol, 1 eq.) is dissolved in 25% aqueous KOH and refluxed for 17 h. Then, the solution is cooled down to room temperature, previously to the addition, in only one portion, of iodomethane (440.0 µL, 6.8 mmol, 1 eq.) and stirred for an additional hour at room temperature. The crude is extracted with diethyl ether and isolated by flash column chromatography on silica gel (hexane / ethyl acetate 7:3) as a green oil in 52% yield.

R_f = 0.320 (hexane / ethyl acetate 7:3).

Yield = 52% (947.6 g, 3.5 mmol).

^{1}H-NMR (300 MHz, $CDCl_3$): δ (ppm) 6.93 (d, *J* = 2.6 Hz, 1H), 6.80 – 6.65 (m, 2H), 3.75 (s, 3H), 2.39 (s, 3H).

1.2. Synthesis of aryldiazonium salts:

1.2.1. Procedure A

Aryldiazonium tetrafluoroborate derivatives are synthesized according to the procedure described by Youn et al. and spectroscopic data are in agreement with the reported values. [3]

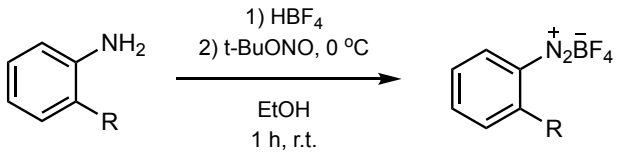

Figure 3 Reaction scheme for the synthesis of aryldiazonium salts.

These compounds are obtained by nitrosation of aniline derivative using *tert*-butyl nitrate in acidic media. With this purpose, aniline (1 eq.) and tetrafluoroboronic acid (2 eq.) are dissolved in ethanol and the mixture is cooled down to 0 °C. *Tert*-butyl nitrate (2 eq.) is added dropwise and the resulting solution is stirred during 1 h at room temperature to afford a solid product after precipitation with diethyl ether.

1.2.2. Procedure B

p-Methoxyaryldiazonium tetrafluoroborate derivatives are synthesized according to the procedure described by Youn et al. and spectroscopic data are in agreement with the reported values. [3]

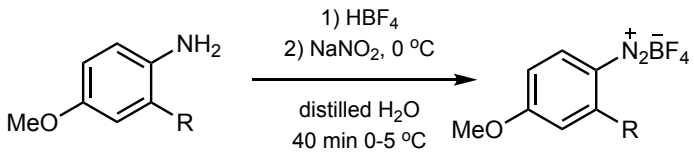

Figure 4 Reaction scheme for the synthesis of para-metoxi aryldiazonium salts.

The compounds are obtained by nitrosation of aniline derivative using sodium nitrate in acidic media. With this purpose, aniline (1 eq.) and tetrafluoroboronic acid (2 eq.) are dissolved in distilled water and the mixture is cooled down until 0 °C. Tert-butyl nitrate (2 eq.) is added dropwise and the resulting solution is stirred during 40 min at 0-5 °C temperature to afford a solid product after filtration. The solid is re-dissolved in acetone and precipitated with diethyl ether to obtain the final product.

ANNEX II

Table 1 Yields obtained for the synthesis of the different aryldiazonium tetrafluoroborate salt derivates.

Compound	Name	R group	Yield%	Colour
3	*Biaryldiazonium tetrafluoroborate salt*	Ph	70%	Light yellow
6a	*2-(Methylthio)benzenediazonium tetrafluoroborate salt*	SMe	96%	Intense yellow
6b	*4-Methoxy-2-(methylthio) benzenediazonium tetrafluoroborate salt*	SMe	97%	Light green
10	*4-Methoxybenzenediazonium tetrafluoroborate salt*	H	80%	Purple

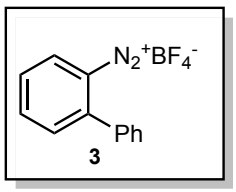

3

^{1}H-NMR (300 MHz, DMSO): δ (ppm) 8.91 (d, ^3J = 8.3 Hz, 1H), 8.35 (t, ^3J = 7.1 Hz, 1H), 8.12 – 7.96 (m, 2H), 7.92-7.82 (m, 2H), 7.74 – 7.65 (m, 3H).

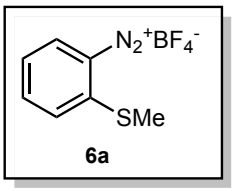

6a

^{1}H-NMR (300 MHz, DMSO): δ (ppm) 8.66 (d, ^3J = 8.3 Hz, 1H), 8.15 (t, ^3J = 7.9 Hz, 1H), 7.97 (d, ^3J = 7.4 Hz, 1H), 7.71 (t, ^3J = 7.9 Hz, 1H), 2.84 (s, 3H).

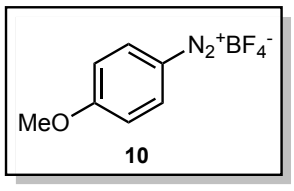

10

^{1}H-NMR (300 MHz, DMSO): δ (ppm) 8.62 (d, ^3J = 8.8 Hz, 2H), 7.49 (d, ^3J = 7.4 Hz, 2H), 4.04 (s, 3H).

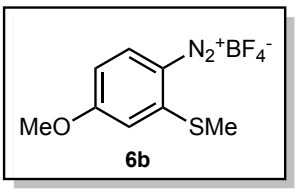

[1]H-NMR (300 MHz, DMSO): δ (ppm) 8.58 (d, ^3J = 9.3 Hz, 1H), 7.32 (d, ^3J = 2.3 Hz, 1H), 7.27 (dd, ^3J = 9.3, 2.3 Hz, 1H), 4.09 (s, 3H), 2.85 (s, 3H).

1.3. Synthesis of alkynoates:

*1.3.1. Synthesis of 2,3,6,7-tetrahydro-1H,5H-pyrido[3,2,1-ij]quinoline-9-yl 3-phenylpropiolate (**9**)*

Alkynoate **9** is synthesized following the procedure described by Vidal et al. and spectroscopic data are in agreement with the reported values. [4]

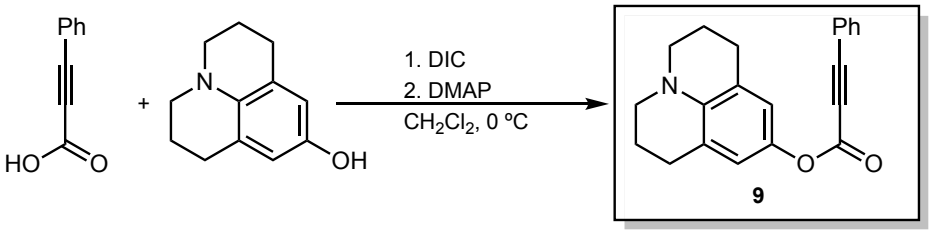

*Figure 5 Reaction scheme for synthesis of compound **9**.*

Phenyl propiolic acid (200.0 mg, 1.1 mmol, 1 eq.) is added to a heat gun dried round bottom flask equipped with stir bar under nitrogen and dissolved with dichloromethane (1.6 mL). The resulting solution is stirred at 0 °C in an ice/brine bath for 1 min. Then, DIC (N,N-dicyclohexylcarbodiimide, 250.0 µL, 1.6 mmol, 1.5 eq.) is added causing the precipitation of a white solid. The mixture is stirred for a minute before addition of solution of 8-hydroxyjulolidine (200.0 mg, 1.4 mmol, 1.3 eq.) in dichloromethane (2.5 mL) followed by addition of 4-(dimethylamino)pyridine (DMAP, 32.0 mg, 1.05 mmol, 0.25 eq.) in dichloromethane (250.0 µL) that turns solution into orange. Final mixture is stirred until consumption of 8-hydroxyjulolidine is observed by TLC. Finally, the reaction mixture is filtered through Kieselguhr, concentrated under vacuum and the final product is obtained after flash column chromatography (hexane / acetate 8:2) yielding product **9** as an orange solid.

Rf = 0.300 (hexane / ethyl acetate 8:2).

Yield = 54% (175.0 mg, 0.6 mmol).

^{1}H-NMR (300 MHz, $CDCl_3$): δ (ppm) 7.63 (d, ^3J = 8.3 Hz, 2H), 7.48 (t, ^3J = 7.5 Hz, 1H), 7.40 (t, ^3J = 7.7 Hz, 2H), 6.81 (d, ^3J = 8.1 Hz, 1H), 6.34 (d, ^3J = 7.9 Hz, 1H), 3.14 (q, ^3J = 5.7 Hz, 4H), 2.75 (t, ^4J = 6.5 Hz, 2H), 2.65 (t, ^3J = 6.6 Hz, 2H), 1.97 (m, 4H).

2. SYNTHESIS OF PRODUCTS

2.1. Synthesis of phenanthrenes:

The procedure is adapted from Zhou et al. and ^{1}H NMR is in concordance with the data reported in the literature. [5]

2.1.1. Representative general procedure for experiments at 330 mM

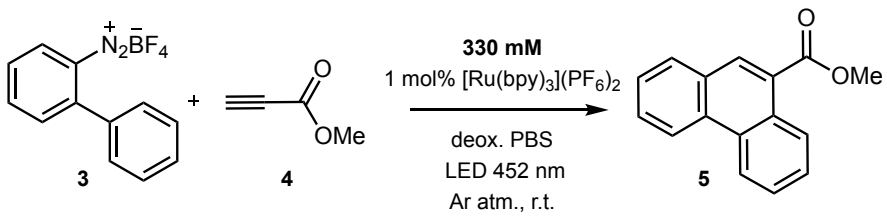

*Figure 6 Scheme of reaction conditions for biaryldiazonium salt **3** concentration of 330 mM.*

In an 8.0 mL glass vial equipped with magnetic stirring bar, biaryldiazonium tetrafluoroborate salt **3** (53.60 mg, 0.2 mmol, 1 eq.) and $[Ru(bpy)_3(PF_6)_2]$ (1.71 mg, 0.002 mmol, 0.01 eq.) are introduced and degassed by vacuum-nitrogen cycles (x3) via a syringe needle. The vial is sealed under an argon atmosphere and the mixture is dissolved in deoxygenated PBS (0.6 mL). Then, methyl propiolate **4** (89.0 µL, 1 mmol, 5 eq.) is added via Hamilton syringe and the vial is irradiated with blue LED lamp (452 nm).

After irradiation, the crude is diluted with water and the aqueous phase is extracted with ethyl acetate (3 x 30.0 mL). The combined organic layers are dried over $MgSO_4$, filtered and concentrated under reduced pressure. The final residue is purified by flash chromatography on silica gel (hexane / ethyl acetate 9:1). During the optimization process, the crude is analysed by ^{1}H NMR. The yield is determined by ^{1}H NMR using nitromethane as internal standard.

R_f = 0.34 (hexane / ethyl acetate 9:1).

^{1}H-NMR (300 MHz, $CDCl_3$): δ (ppm) 8.98 – 8.87 (m, 1H), 8.78 – 8.65 (m, 2H), 8.48 (s, 1H), 7.97 (d, ^3J = 7.9 Hz, 1H), 7.81 – 7.58 (m, 4H), 4.06 (s, 3H).

LR-MS Calculated for $[C_{16}H_{13}O_2]^+$: 237.09; found: 236.80.

2.1.2. Representative general procedure for experiments at 10 mM

In case of 10 mM experiments, similar protocol is used but a catalyst loading of 5 mol% of $[Ru(bpy)_3(PF_6)_2]$ is used instead of 1 mol% instead of 1 mol%.

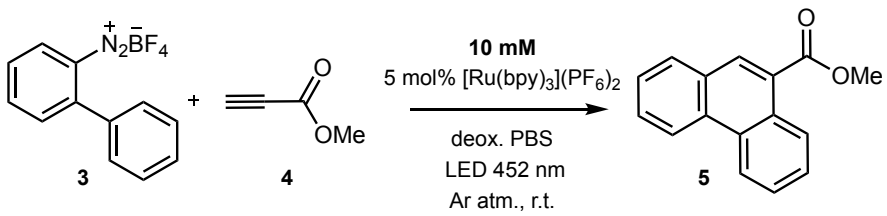

*Figure 7 Scheme of reaction conditions for biaryldiazonium salt **3** concentration of 10 mM.*

*2.1.3. General procedure for slow addition of diazonium salt **3** exemplified for experiments at 10 mM*

The stock solution is prepared by dissolving biaryldiazonium salt **3** (26.8 mg, 0.1 mmol) in PBS (400 µL) inside an Eppendorf (1mL). Then, 200 µL of the solution are added via syringe into the sealed vial, containing the reactants left, and using an automatic pump machine with addition rate of 0.04 mL/min in order to ensure the continuous and slow addition as well as the reproducibility of the process.

2.1.4. Study of the reaction under biological relevant conditions

In experiments carried out in complex biological media, standard conditions have been followed at 10 mM. The reaction is studied in different biological media:

-Gibco DEMEM (Dubelcco's Modified Eagle's Medium) purchased from *ThermoFisher Scientific*.

-Bovine serum albumin (BSA) obtained from Sigma Aldrich and dissolved in PBS until getting a final concentration of 5 mg/mL.

-HeLa cell lysates, obtained from 2 days cultured HeLa cells: after two washings with PBS, cells are scraped from the well, sonicated and diluted with PBS to reach the concentration of 1.03 cell lysates/mL.

-Suspension of HeLa cells. The cells are cultured and suspended in PBS to achieve the concentration of 5 mg/mL.

2.2. Synthesis of benzotiophenes:

2.2.1. Representative general procedure for experiments at 250 mM in DMSO

Benzotiophene derivatives are synthesized according to the procedure described by König et al. and spectroscopic data are in agreement with the reported values. (2)

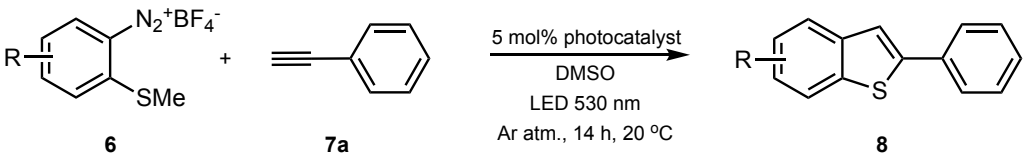

6 **7a** **8**

*Figure 8 Scheme of reaction conditions for a concentration of aryldiazonium salt **6** equal to 250 mM.*

In an 8.0 mL glass vial equipped with a magnetic stirring bar, aryldiazonium tetrafluoroborate salt **6** (0.25 mmol, 1 eq.) and photocatalyst (0.0125 mmol, 0.05 eq.) are introduced and degassed by vacuum-nitrogen cycles (x3) via a syringe needle. The vial is sealed under an argon atmosphere and the mixture is dissolved in deoxygenated dimethylsulfoxide (1.0 mL). Then, phenylacetylene **7a** (1.25 mmol, 5 eq.) is added and the vial is irradiated with green LED lamp (530 nm). After irradiation, the crude is diluted with diethyl ether, washed with water and the aqueous phase is extracted with diethyl ether (3 x 30.0 mL). The combined organic layers are dried over $MgSO_4$, filtered and concentrated under reduced pressure. The final residue is purified by flash chromatography on silica gel. During the optimization process, the crude is analysed by ^{1}H NMR. The yield is determined by ^{1}H NMR using nitromethane as internal standard.

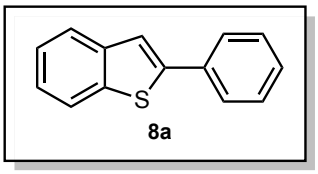

8a

R_f = 0.51 (hexane).

^{1}H-NMR (300 MHz, $CDCl_3$): δ (ppm) 7.84 (d, ^3J = 8.1 Hz, 1H), 7.78 (d, ^3J = 7.2 Hz, 1H), 7.73 (d, ^3J = 8.2 Hz, 2H), 7.55 (s, 1H), 7.49-7.40 (m, 2H), 7.40-7.28 (m, 3H).

LR-MS Calculated for $[C_{14}H_{11}S]^+$: 211.05; found: 210.81.

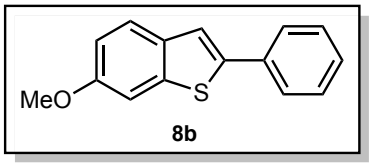

8b

R_f = 0.34 (hexane / ethyl acetate 9:1).

^{1}H-NMR (300 MHz, $CDCl_3$): δ (ppm) 7.73-7.62 (m, 3H), 7.47 (s, 1H), 7.46-7.37 (m, 2H), 7.37-7.27 (m, 2H), 6.98 (dd, ^3J = 8.7, 2.4 Hz, 1H), 3.89 (s, 3H).

LR-MS Calculated for $[C_{15}H_{13}OS]^+$: 241.06; found: 240.80.

When PBS is used as reaction media (1.0 mL), a different work-up must be performed. The crude is diluted with water and the aqueous phase is extracted with ethyl acetate (3 x 30.0 mL). The combined organic layers are dried over $MgSO_4$, filtered and concentrated under reduced pressure to obtain the final product.

Finally, for experiments with different catalytic loading, the amount of catalyst is changed while keeping all the other conditions.

2.3. Synthesis of coumarins:

The procedure is adapted from Ji et al. [6]

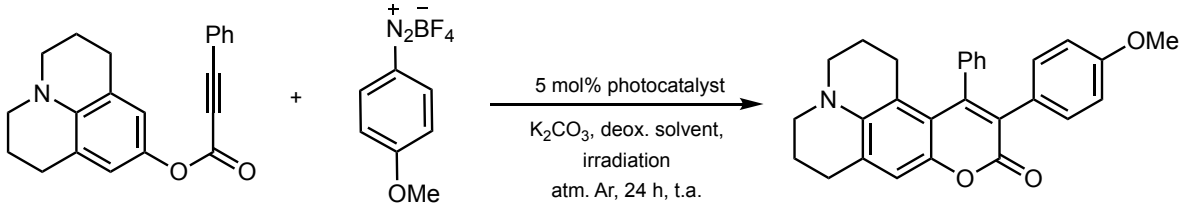

9 **10** **11**

*Figure 9 Scheme of reaction conditions for the synthesis of coumarin **11**.*

In an 8.0 mL glass vial equipped with magnetic stirring bar, alkynoate **9** (0.25 mmol, 2.5 eq.), 4-methoxyaryldiazonium salt **10** (0.1 mmol, 1 eq.), photocatalyst (0.005 mmol, 0.05 eq.) and K_2CO_3 (0.1 mmol, 1 eq.) are introduced and degassed by vacuum-nitrogen cycles (x3) via a syringe needle. The vial is sealed under argon atmosphere and the mixture is dissolved in deoxygenated solvent (1.0 mL). Then, the vial is irradiated with suitable LED lamp during 24 h at room temperature. The reaction is followed by TLC (hexane / ethyl acetate 8:2) to completion of reactants. The crude of the reaction is subjected to suitable work-up to get the final product.

2.4. Preliminary reactions in cellular settings

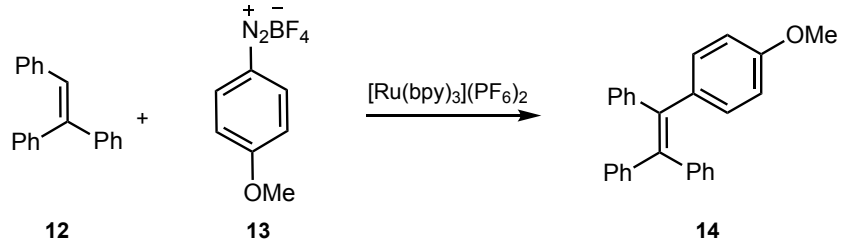

*Figure 10 Scheme of reaction conditions for AIE fluorophore **14** formation.*

First, two days before treatment, HeLa cells are seeded on 12 well plates. Then, cells are incubated with the ruthenium complex $[Ru(bpy)_3](PF_6)_2$ (50 µM) for 30 min in fresh DMEM. After 30 min, in order to remove extracellular ruthenium complex, two washing steps are needed (400 µM of DEMEM) . Resulting cells are incubated with substrates **12** and **13** (100 µM each) in fresh DMEM for 20 min to ensure intracellular reaction.

In parallel, control experiments are performed by incubation of either [Ru] or substrates **12** and **13** in DEMEM for 30 and 20 min, respectively. Then, cells are irradiated at 460 nm for 10 min with the laser of the microscope before observation under the epifluorescence microscope (I_{exc}= 385 nm and I_{em}=450 nm). The digital pictures of the different samples were taken under identical conditions of gain and exposure under epifluorescence microscope.

ANNEX III

1. SUBSTRATES: ^{1}H-NMR SPECTRA.

1.1. ^{1}H-NMR spectra for aniline derivatives 1 and 2

*1.1.1. ^{1}H-NMR spectra of 2-(methylthio)aniline **1**.*

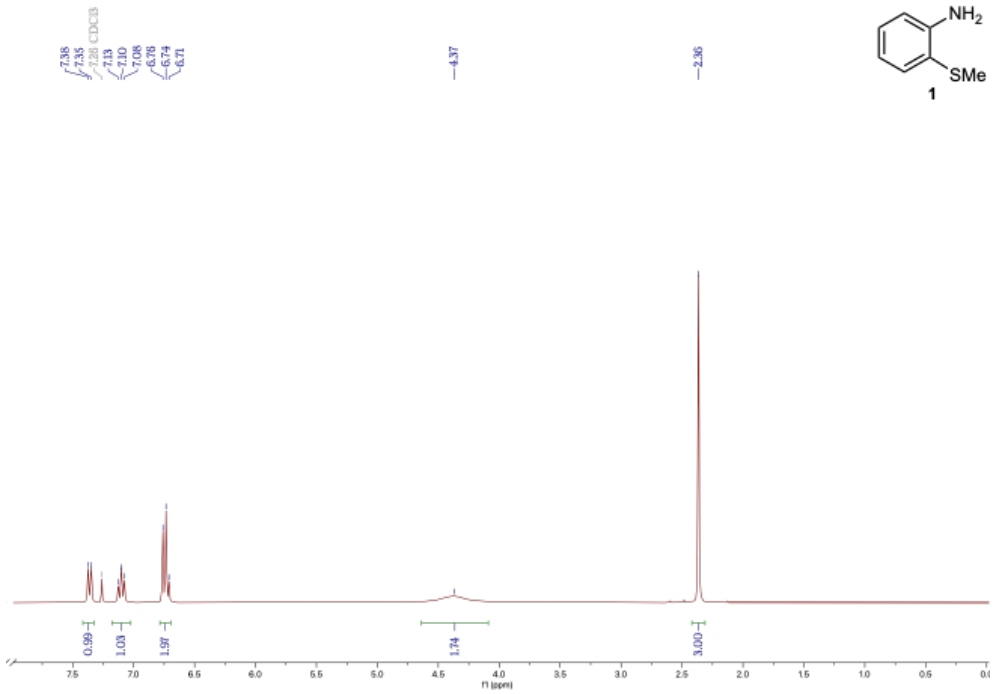

*1.1.2. ^{1}H-NMR spectra of 4-methoxy-2-(methylthio)aniline **2**.*

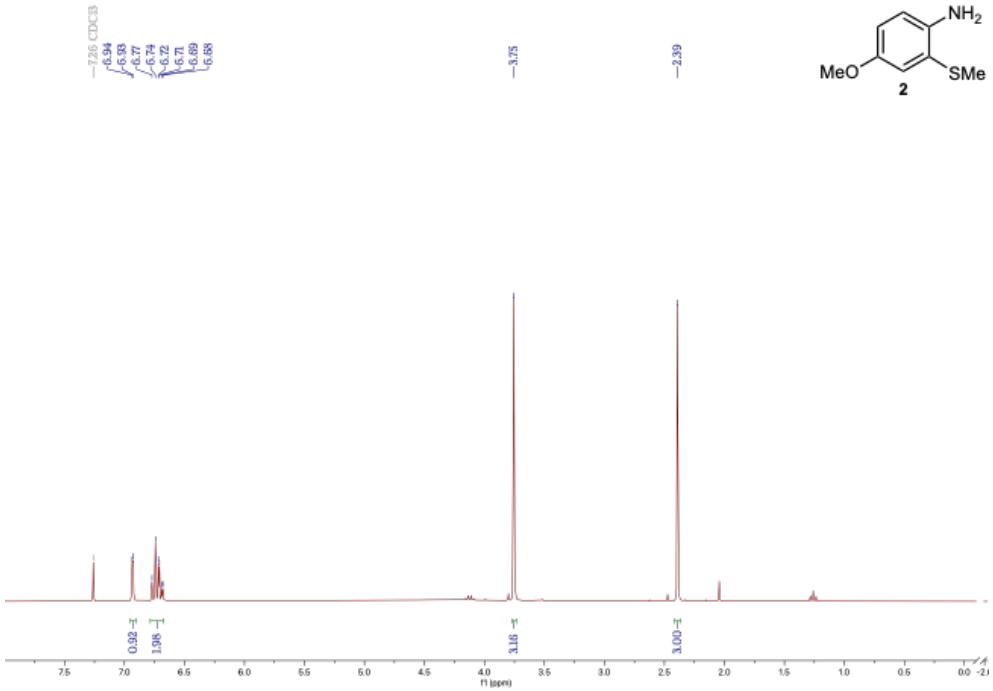

1.2. ^{1}H-NMR spectra for aryldiazonium salts 3, 6a, 6b and 10:

*1.2.1. ^{1}H-NMR spectra of 2-phenylbenzenediazonium tetrafluoroborate **3**:*

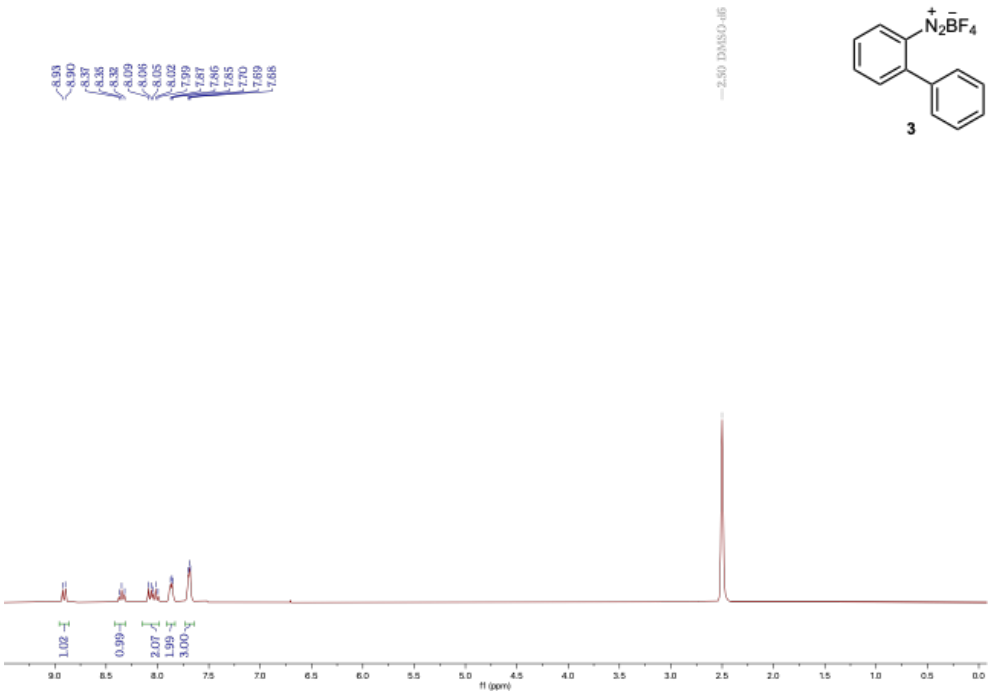

*1.2.2. ^{1}H-NMR spectra of 2-(methylthio)benzenediazonium tetrafluoroborate **6a**:*

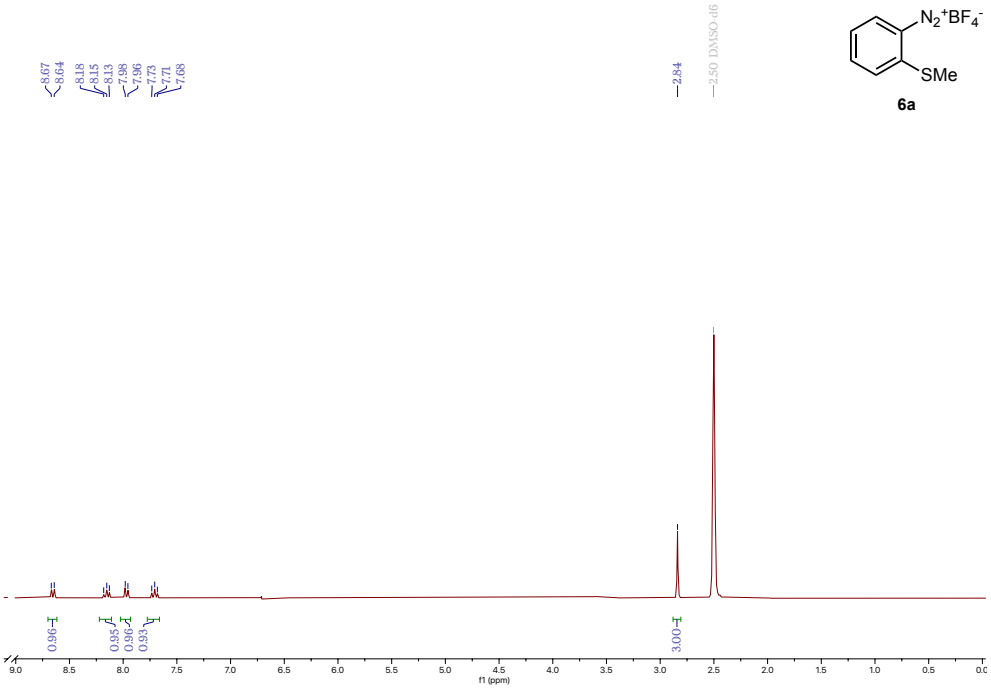

*1.2.3. ^{1}H-NMR spectra of 4-methoxy-2-(methylthio)-benzenediazonium tetrafluoroborate **6b**:*

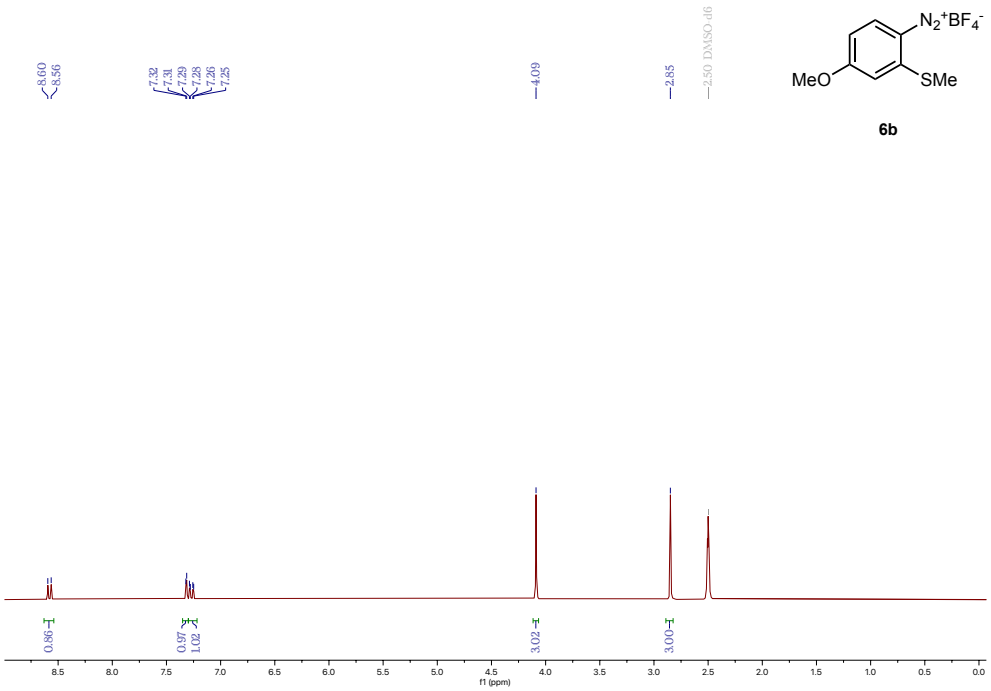

*1.2.4. ^{1}H-NMR spectra of p-methoxybenzenediazonium tetrafluoroborate **10**:*

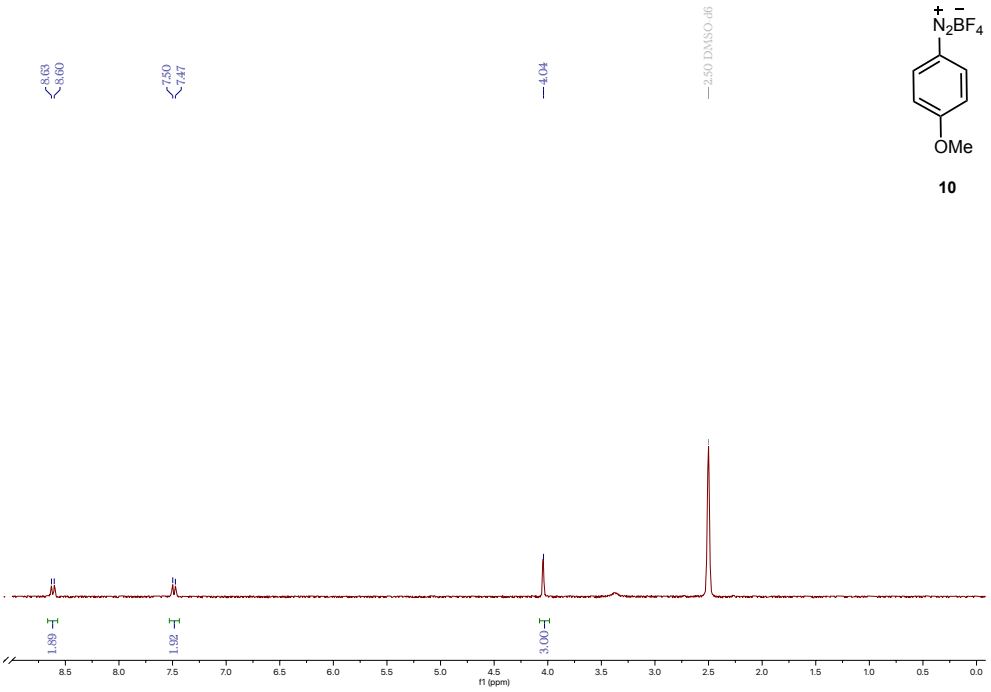

1.3. ^{1}H-NMR spectra for alkynoate derivative 9.

*1.3.1. ^{1}H-NMR spectra of 2,3,6,7-tetrahydro-1H,5H-pyrido[3,2,1-ij]quinoline-8-yl 3-phenylpropiolate **9**.*

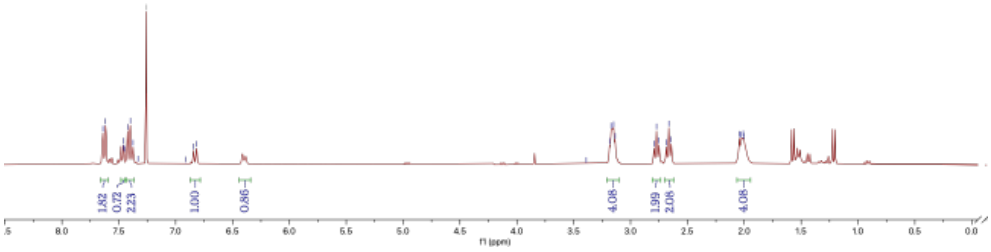

2. PRODUCTS: ^{1}H-NMR SPECTRA.

2.1. ^{1}H-NMR spectra for phenanthrene 5.

*2.1.1. ^{1}H-NMR spectra of methyl phenanthrene-9-carboxylate **5**.*

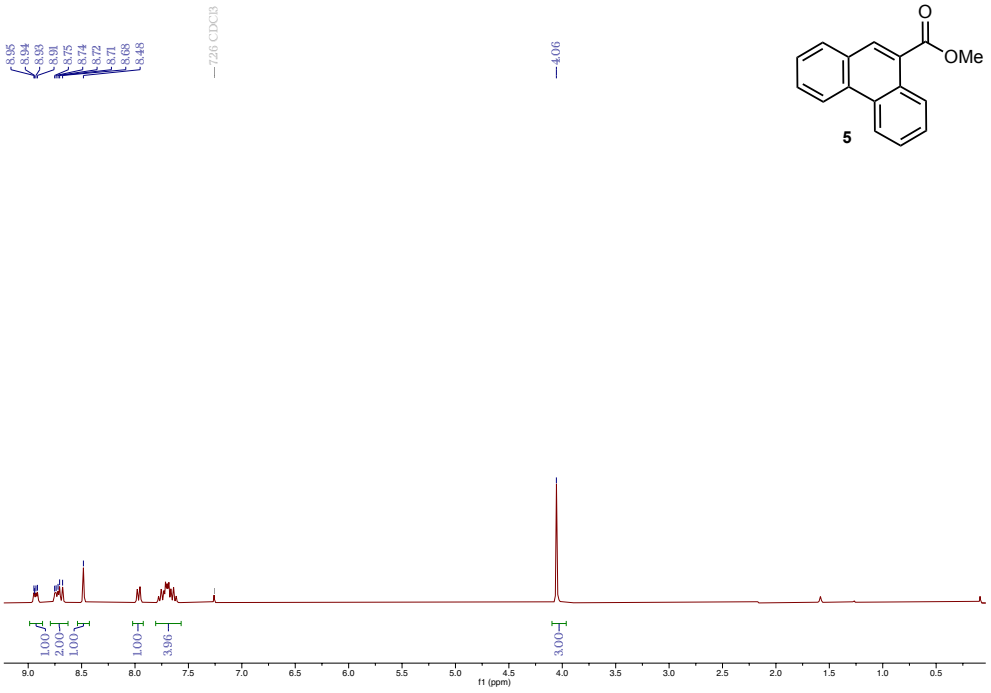

2.2. ^{1}H-NMR spectra for benzotiophenes 8a and 8b:

*2.2.1. ^{1}H-NMR spectra of 2-phenylbenzo[b]tiophene **8a**:*

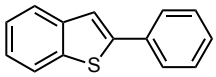

8a

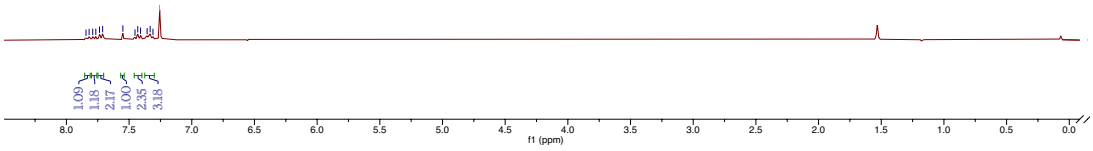

*2.2.2. ^{1}H-NMR spectra of 6-methoxy-2-phenylbenzo[b]tiophene **8b**:*

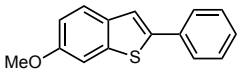

8b

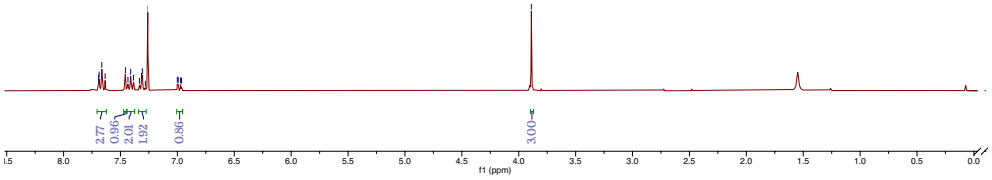

ANNEX IV

1. ANALITICAL METHODOLOGY

1.1. Internal standard method

^{1}H-NMR spectra is used for quantifying the yield by comparing a singular signal of the desired product with the corresponding signal for an internal standard. The internal standard must be chosen carefully, taking into account that it should behave similarly to the analyte of interest.

This method is used for determining the yield of phenanthrene and benzotiophene formation. In both cases, nitromethane in $CDCl_3$ is used as an internal standard and the amount of nitromethane needed is calculated for each substrate concentration (330 mM or 10 mM for phenanthrenes and 250 mM for benzotiophenes) so that for 100% yield, the relation between the signals of nitromethane and metoxi group is 1:3 (*Table 1*). Consequently, from the relation between both signals, yield can be estimated.

Substrate	mmol	[Nitromethane]/ µL mL^{-1}
1	0.20	3.67
1	0.05	0.94
4b	0.25	4.7

Table 2 Concentration of nitromethane as a function of mmol of the substrate used.

On the one hand, for phenanthrene formation, we calculate the relation between the signal for nitromethane (δ = 4.32 ppm) and that for the metoxi group (δ = 4.05 ppm) to get the yield as shown in *figure 1*. Moreover, we can also use two signals (8.9 ppm and 8.5 ppm) that ideally integrate by 1H, therefore the yield is given as an average of the three values.

$$\%Yield = \frac{1.82/3 + 0.59 + 0.61}{3} x\ 100 = 60.2\%$$

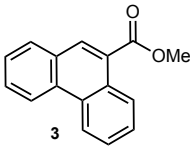

3

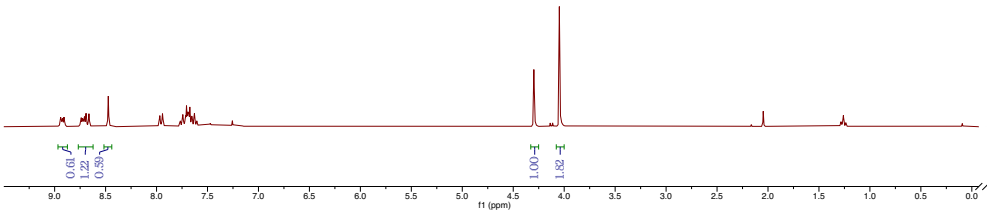

Figure 11 Example of yield's calculation for phenanthrene formation.

On the other hand, for benzotiophenes formation, we simply calculate the relation between the signal for nitromethane (δ= 4.32 ppm) and that for the metoxi group (δ= 3.89 ppm) to get the yield as shown in *figure 2.*

$$\%Yield = \left(\frac{1.12}{3}\right) x\ 100 = 37.3\%$$

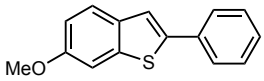

6b

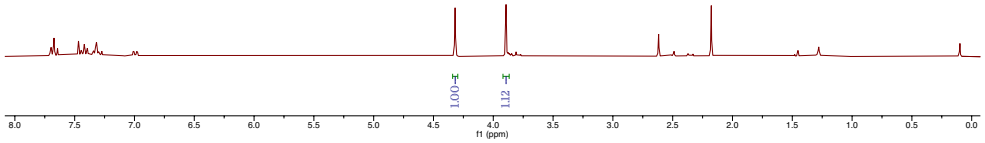

Figure 12 Example of yield's calculation for benzotiophene formation.

ANNEX V

1. INSTRUMENTATION

1.1. Photoreactor.

One of the big drawbacks of photochemical methods is the difficulty related to standardization and reproducibility of the results. In order to get suitable and reproducible results is fundamental to control several parameters, mainly: the intensity of the radiation source, the uniformity of the optical pathway through the sample, the stirring intensity and the temperature. [7]

The photoreactor used in this project is *HepatoChem EvoluChem™ PhotoRedOx Box (HepatoChem Box*). This instrument requires an external radiation source and samples are irradiated through a mirror system. This issue has a main advantage: as long as the lamp is available, any radiation (any λ) can be used, but the intensity can only be controlled if it has its own control system. The refrigeration system consists on a fan that indirectly cools down the reactions vessels and it is located at the bottom of the photoreactor. Nevertheless, there is also a liquid cooled system available, but it was not used for this project. Concerning the stirring system, this is external too and it basically consist on a common magnetic stirring plate located just under the photoreactor to get a suitable agitation of the reaction samples.

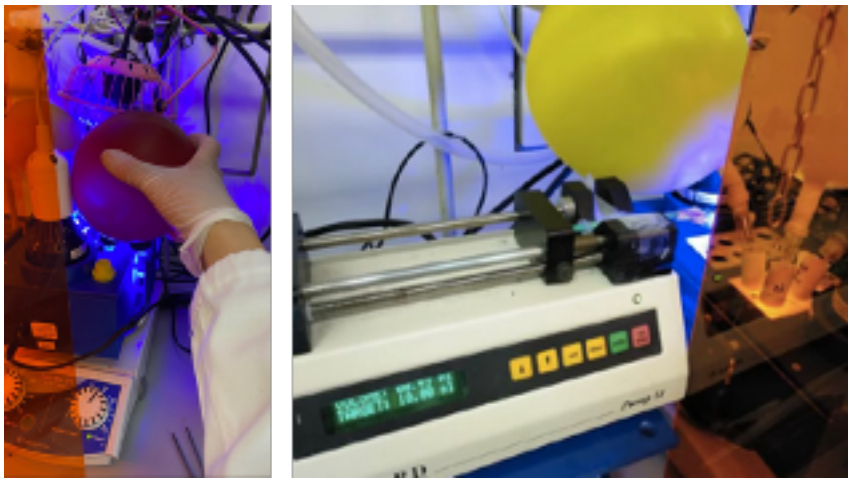

Figure 13 Set-up for photochemical methods.

REFERENCES

1. Basak, D.; Leusen, J.; Gupta, T.; Kögerler, P.; Bertolasi, V. and Ray, D. (2020) Unusually distorted pseudo-octahedral coordination environment around Co^{II} from thioether shiff base ligands in dinuclear [CoLn] (Ln=La, Gd, Tb, Dy, Ho) complexes: synthesis, structure and understanding of magnetic behaviour. *Inorg. Chem*., **59**, 2387-2405.

2. Hari, D. P.; Hering, T. and König, B. (2012) Visible light photocatalytic synthesis of benzotiophenes. *Org. Lett.*, **4**, 5334-5337.

3. Lee, M. E. and Youn, W. S. (2016) Metal-free one-pot synthesis of N,N'-diarylamidines and N-arylbenzimidazoles from arenediazonium salts, nitriles and free anilines. *Org. Lett.*, **18**, 5728-5731.

4. Vidal, C.; Tomás-Gamasa, M.; Destito, P.; López, F. and Mascareñas, J. L. (2018) Concurrent and orthogonal gold (I) and ruthenium (II) catalysis inside living cells. *Nat. Commun.*, **9**, 1913.

5. Xiao, T.; Dong, X.; Tang, Y., and Zhou, L. (2012) Phenanthrene synthesis by eosin-Y-catalyzed visible light induced [4+2] benzannulation of biaryldiazonium salts with alkynes. *Adv. Synth. Catal*., **354**, 3195-3199.

6. Fu, W.; Zhu, M.; Zou, G.; Xu C.; Wang, Z. and Baoming, J. (2015) Visible-light mediated radical aryldifluoroacetylation of alkynes with ethyl bromodifluoroacetate for the synthesis of 3-difluoroacetylated coumarins. *Org. Chem.,* **80**, 4776-4770.

7. Svejestrup, T.D.; Chatterjee, D. S.; Wagner, T.; Zach, J.; Johansson, M. J.; Bergozini, G. and König, B. (2021). Effects of light intensity and reaction temperature on photoreactions in commercial photoreactors. ChemPhotoChem, **5**, 1-8.